remote sensing

MDPI

Article

Landscape Change Detected over a Half Century in the Arctic National Wildlife Refuge Using High-Resolution Aerial Imagery

Janet C. Jorgenson [1,*], M. Torre Jorgenson [2], Megan L. Boldenow [3] and Kathleen M. Orndahl [4]

1 U. S. Fish & Wildlife Service, Fairbanks, AK 99701, USA
2 Alaska Ecoscience, Fairbanks, AK 99709, USA; ecoscience@alaska.net
3 Department of Biology and Wildlife, University of Alaska, Fairbanks, AK 99775, USA; mboldenow@gmail.com
4 School of Informatics, Computing & Cyber Systems, Northern Arizona University, Flagstaff, AZ 86011, USA; kmo265@nau.edu
* Correspondence: janet_jorgenson@fws.gov; Tel.: 1-907-456-0250

Received: 2 June 2018; Accepted: 27 July 2018; Published: 18 August 2018

Abstract: Rapid warming has occurred over the past 50 years in Arctic Alaska, where temperature strongly affects ecological patterns and processes. To document landscape change over a half century in the Arctic National Wildlife Refuge, Alaska, we visually interpreted geomorphic and vegetation changes on time series of coregistered high-resolution imagery. We used aerial photographs for two time periods, 1947–1955 and 1978–1988, and Quick Bird and IKONOS satellite images for a third period, 2000–2007. The stratified random sample had five sites in each of seven ecoregions, with a systematic grid of 100 points per site. At each point in each time period, we recorded vegetation type, microtopography, and surface water. Change types were then assigned based on differences detected between the images. Overall, 23% of the points underwent some type of change over the ~50-year study period. Weighted by area of each ecoregion, we estimated that 18% of the Refuge had changed. The most common changes were wildfire and postfire succession, shrub and tree increase in the absence of fire, river erosion and deposition, and ice-wedge degradation. Ice-wedge degradation occurred mainly in the Tundra Biome, shrub increase and river changes in the Mountain Biome, and fire and postfire succession in the Boreal Biome. Changes in the Tundra Biome tended to be related to landscape wetting, mainly from increased wet troughs caused by ice-wedge degradation. The Boreal Biome tended to have changes associated with landscape drying, including recent wildfire, lake area decrease, and land surface drying. The second time interval, after ~1982, coincided with accelerated climate warming and had slightly greater rates of change.

Keywords: Alaska; Arctic; tundra; boreal; climate change; shrub increase; aerial photography; remote sensing; vegetation; permafrost; thermokarst; fire

1. Introduction

The Arctic National Wildlife Refuge (hereafter, Refuge) in northeastern Alaska spans from the Beaufort Sea coast and coastal plain tundra across the high Brooks Range to the boreal forest. It covers 80,324 km^2 and is the largest protected conservation area in the United States. The Refuge encompasses a wide temperature range and a diversity of ecosystems and, thus, is a natural laboratory for evaluating climate change impacts. Because the Refuge is very remote, with no roads and few airstrips, we used high-resolution imagery to remotely sense geomorphic and vegetative changes over a ~50-year period.

The arctic climate has warmed rapidly during the past 50 years, with annual average temperatures increasing nearly twice as fast as the world average [1]. The rate of warming in Alaska rose sharply beginning in 1977, concurrent with large-scale atmosphere and ocean regime shifts, such as the Pacific Decadal Oscillation [2–4], and warming has continued since then [5,6].

Most evidence for landscape change in the Arctic comes from remote sensing, mainly automated processing of satellite images at 30-m (LANDSAT) to 1-km resolution (AVHRR), because of the vast remote areas [7,8]. The normalized difference vegetation index (NDVI), an index of quantity of green vegetation derived from satellite data, has increased Arctic-wide since the 1970s, with the greatest increases in northern Alaska [9–11]. The increase has generally been attributed to broad-scale increases in shrubs [12–15]. There can be considerable spatial heterogeneity, however, depending on remote sensing technique and scale. Bhatt et al. [16] used AVHRR to reveal that trends in the summer warmth index (sum of degree months above freezing) from 1982 to 2011 varied by region, with summer warmth index increasing over time in northern Alaska. Pattison et al. [17] found little change in NDVI from 1984 to 2009 in the northern portion of the Refuge, corresponding with little change in ground monitoring plots. Using high-resolution Landsat data (1985–2007) to detect NDVI trends in the foothills of northern Alaska, Raynolds et al. [18] found both significant increases and decreases across the heterogeneous terrain.

Ground-based data documenting change in Alaska and the Arctic have been accumulating rapidly. Elmendorf et al. [19] synthesized vegetation changes over time in plots across the Arctic and found a widespread trend of increasing shrub abundance. Plots from that synthesis that were from the Refuge showed patchy change but no trend, with only one of 27 plots showing shrub increase and three with augmented ice-wedge degradation between 1984 and 2009 [20]. Other studies documented increasing ice-wedge degradation [21] and wildfire [22,23] in Alaska in recent decades.

More work is needed at high-resolution scales to relate results from large-scale remote sensing studies to small-scale field studies. For example, there is a mismatch between the many remote sensing studies that indicate a wide-spread shrub invasion of Arctic tundra and local field-based observations suggesting that the changes are less dramatic, more complex, and heterogeneous. Manual photointerpretation of high-resolution (<4 m) images provides that high-resolution scale but is limited to smaller areas due to cost, time, and data-processing load. Yet manual image interpretation of high-resolution imagery has many advantages. It can detect both geomorphic changes (e.g., ice-wedge degradation, channel migration) and vegetation structural changes (e.g., tree and tall shrub changes evident from shadows), it allows for comparison among vastly different image types (e.g., black and white and color-infrared (CIR) aerial photos, satellite imagery), and its ability to detect change is improved by the expertise and experience of the photointerpreter. A disadvantage is that consistency between observers, or for one observer working on different landscape types, is not assured.

Interpretation of repeat aerial photography and satellite imagery has long been used to quantify landscape and vegetation changes that have occurred since the 1950s. Surface waterbody decreases in subarctic Alaska have been documented by manual image interpretation [24] and in western Alaska by automated classification of imagery [25]. For changes not involving waterbodies, such as the following examples, change detection has usually been done by manual interpretation of images. Increases in shrub cover have been observed at some northern Alaska tundra sites between the 1950s and present [26–28]. Photointerpretation of time-series imagery also has been used to quantify recent increases in thermokarst associated with collapse-scar fens [29], ice-wedge degradation [21,30], and thaw slumps [31]. These studies often focused on small rapidly changing areas, so are of limited use for assessing changes over larger regions. We addressed this limitation by using a random-systematic sampling design to estimate changes across the entire Refuge and its diverse ecosystems.

Our objectives were to: (1) document geomorphic and vegetative changes across the entire Arctic National Wildlife Refuge since the 1950s; (2) quantify the amount of change in seven ecoregions of the Refuge; and (3) compare rates of change between early and recent intervals of the study (before and after ~1982). We used visual interpretation to document landscape change at points located on multiple time series of coregistered aerial images, which consisted of panchromatic aerial photographs from 1947 to 1955, CIR aerial photographs from 1978 to 1988, and high-resolution, multispectral satellite images (Quick Bird, IKONOS) from 2000 to 2007. We undertook this study with a view to validating global change models and predicting future changes based on climate modelling.

2. Materials and Methods

2.1. Study Area

The Refuge spans from the Beaufort Sea coast in the north, across the Brooks Range to the boreal forest and tributaries of the Yukon River in the south. Our study area thus extended across Tundra, Mountain, and Boreal Biomes. Table 1 summarizes geographic and temperature data. The mean annual temperature is below freezing and all parts of the Refuge are underlain by continuous permafrost except for larger river valleys in the far south. Surficial permafrost features such as ice-wedge polygons, beaded streams, peat ridges, and frost boils are common throughout. Vegetation types are summarized in Table A1. There is increasing continental and diminishing maritime influence with distance from the coast. While long-term climate records do not exist for the Refuge, mean annual temperatures have risen 2.0 °C since the 1950s at Barrow, on the Arctic coast, and 2.3 °C at Bettles, in the boreal forest [32]. The greatest warming has occurred during winter and spring. Higher temperatures are causing earlier spring snow melt, reduced sea ice, glacier retreat, insect outbreaks, and permafrost warming [6].

Table 1. Geographic and temperature information for ecoregions of the Arctic Refuge. Size, elevation, and slope are derived from Refuge GIS data and 2005 digital elevation model. Average temperatures (°C) are based on data from nearby weather stations, 1961–1990, and a model that included topographic data (PRISM). Percent burned is from the Alaska Fire Service database.

Biomes & Ecoregions (North to South)	% of Refuge	Area (km^2)	% Burned (1950–2010)	Mean Annual Temp. (°C)	January Temp. (°C)	July Temp (°C)	Mean Elevation (m)	Mean Slope (°)
Tundra Biome:								
Beaufort Sea Coast	1	850	0	−11	−26	6	3	1
Beaufort Coastal Plain	5	3788	0	−11	−26	6	59	1
Brooks Foothills	8	6278	0	−10	−26	9	317	3
Mountain Biome:								
Brooks Range North	31	24,731	0	−8	−25	9	1106	22
Brooks Range South	21	16,488	0	−8	−26	10	1170	18
Boreal Biome:								
Interior Uplands	27	22,064	12	−6	−24	14	633	5
Interior Lowlands	8	6126	58	−5	−26	15	350	3
Whole Refuge	100	80,325	8	−8	−25	11	813	13

The Tundra Biome extends from the Brooks Range in the south to the Arctic Ocean in the north and includes the northern foothills of the Brooks Range, the coastal plain, and the coast of the Arctic Ocean. It has an arctic climate with a short (June to August) growing season and low precipitation. The coastal plain is comprised mainly of undulating moist tundra with vast floodplains and small areas of thaw lake plains. The foothills have rolling hills and plateaus, with better defined drainages. Vegetation is composed mainly of hardy dwarf shrubs, sedges, and mosses. Habitats can be grouped into four broad categories: coastal lagoons, wet sedge tundra and lakes, river floodplains, and upland moist sedge-shrub tundra areas [33].

The Mountain and Boreal Biomes have a continental subarctic climate. Annual precipitation and snow depths exceed those of the Tundra Biome and higher evapotranspiration and warmer summers create drier habitats. The Mountain Biome includes the rugged topography of the Brooks Range. The four highest peaks and the largest glaciers in the range are in the Refuge. Valleys are wide, steep sided, and flat floored, cut by glaciers and then filled with alluvium. Barren rock and sparse, dry alpine tundra predominate. Valleys contain moist sedge-shrub tundra and white spruce woodlands extend up the south-flowing rivers on favorable sites. The Boreal Biome occurs south of the Brooks Range. White and black spruce forests and woodlands predominate in the lowlands, whereas the uplands are rounded ridges with woodlands or open moist sedge-shrub tundra. Frequent, large wildfires shape the vegetation in this biome.

2.2. Sampling Design

Site selection involved regional stratification, image review to identify random sites with time series of suitable imagery, and establishment of sampling grids for photointerpretation. We used a stratified-random sampling design to select five random sites in each of seven ecoregions for a total of 35 study sites (Figure 1).

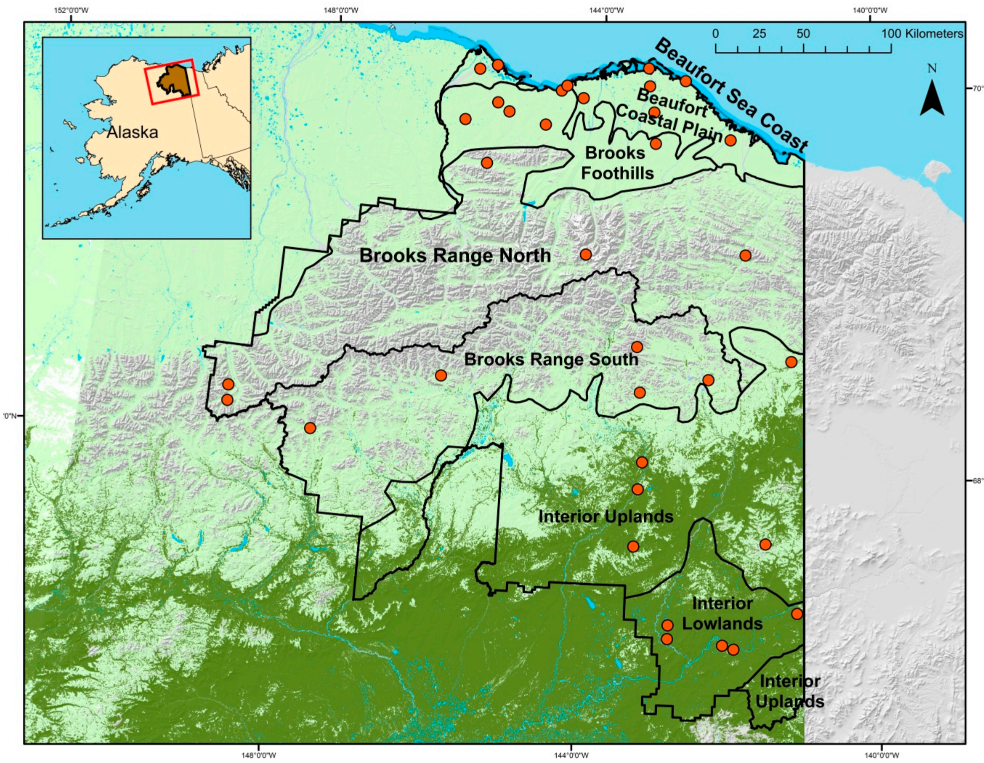

Figure 1. Map of ecoregions of the Arctic National Wildlife Refuge based on Nowacki et al. (2001), with five sites in each ecoregion randomly chosen from area of overlap between acceptable images in all three time periods of the study (red dots).

We defined ecoregions according to Ecoregions of Alaska [34], with minor modifications (Figure 1, Table 1). We separated out a Beaufort Sea Coast ecoregion, defining this as a 300-m wide band stretching the length of the coast, widened as necessary to encompass salt marshes. We also divided the Brooks Range ecoregion into two units north and south of the continental divide. We combined the Davidson Mountains and Ogilvie Mountains ecoregions into a single Interior Uplands ecoregion because they had similar topography and snow-free satellite imagery was not available for the Ogilvie Mountains (1% of Refuge).

To establish the sampling grids, we first generated a set of random locations in each ecoregion. We then went sequentially through the list to identify locations with acceptable images for all three periods (Figure A1). We required all imagery to have greened-up vegetation (generally mid-June to August) and little or no snow cover, clouds, or haze.

2.3. Image Acquisition and Manipulation

Image preparation included image acquisition, enhancement and georeferencing. We acquired and compiled imagery for three sampling periods. Image sources and resolution are listed in Table 2 and extent of available imagery is shown in Figure A1. For the first time period, we used 1947–1950 military aerial photographs, available for 21 of 35 sites, including all sites in the northern four ecoregions and two of five in the southern Brooks Range ecoregion. We used 1955 US Geological Survey aerial photographs for the remaining 14 sites. For the second time period, 1978–1988, we had excellent CIR aerial photograph coverage of the northern part of the Refuge, including a grid of flight lines that spanned most of the Coast, Coastal Plain, and Arctic Foothills ecoregions, repeated in 1984, 1985, and 1988. In addition, we had complete coverage of 1981 true color photographs. For the southern part of the Refuge in this time period, we used CIR aerial photographs from the Alaska High Altitude Project (AHAP). For the third time period, 2000–2007, we acquired map layers showing all Quickbird and IKONOS satellite imagery archived and available for purchase in 2008. We chose the "standard" imagery option, which was geographically referenced and terrain corrected. We recently acquired Worldview satellite images from 2011 to 2014 for some of our grids and used them as additional verification of changes. However, our data and results are from 2000 to 2007 imagery. For the aerial photography, we acquired high-resolution scans of all images for each grid (1200–1800 dpi). The images were either scanned from transparencies (preferred) or prints depending on availability. An example of overlapping images for a site is provided in Figure 2.

Table 2. Aerial photographs and satellite imagery used to detect change in the Arctic National Wildlife Refuge, with source, dates, and resolution.

Image Type	Source	Dates	Color	Scale	Resolution (m)
Aerial Photography	U. S. Air Force	1947	B & W	1:40,000, 1:30,000, 1:12,000	0.3–1.0
Aerial Photography	Naval Arctic Research Laboratory	1948–1950	B & W	1:20,000	0.4–0.6
Aerial Photography	U. S. Geological Survey	1955	B & W	1:50,000	1.0
Aerial Photography	Alaska High-Altitude Photography Program	1978–1982	Color Infrared	1:60,000	1.0
Aerial Photography	U. S. Fish & Wildlife Service	1981	True Color	1:18,000	0.3
Aerial Photography	U. S. Fish & Wildlife Service	1984, 1985, 1988	Color Infrared	1:6,000	0.1
Quickbird Satellite Imagery	Digital Globe	2002–2007	Color (pan-sharpened) & B&W (pan)		0.6 (pan), 2.4 (color)
IKONOS Satellite Imagery	Digital Globe	2000–2006	Color (pan-sharpened) & B&W (pan)		0.8 (pan), 4 (color)
Worldview Satellite Imagery	Digital Globe	2010–2015	True Color (pan-sharpened)		0.3

We produced a time series of spatially aligned images for each 100-point study grid. Image processing was done with ERDAS Imagine software. We pan-sharpened the satellite image by merging the panchromatic and multispectral bands. A portion of each aerial photograph (~2.6 km^2 needed to cover the study grid) was then georeferenced to the satellite image using 15–40 ground control points that were developed from distinct features visible on the images. Stable features were easy to find on most landscape types and included individual trees and shrubs, junctions between ice-wedge polygon troughs, other permafrost features, bird mounds, and boulders. Georeferencing was often difficult on steep mountain slopes with scree and dwarf shrub vegetation, which tended to have fewer distinct and constant points across all images. On steep slopes, we resorted to rectifying different slopes separately or stretching the photo with temporary ground control points as we worked across different parts of the photo.

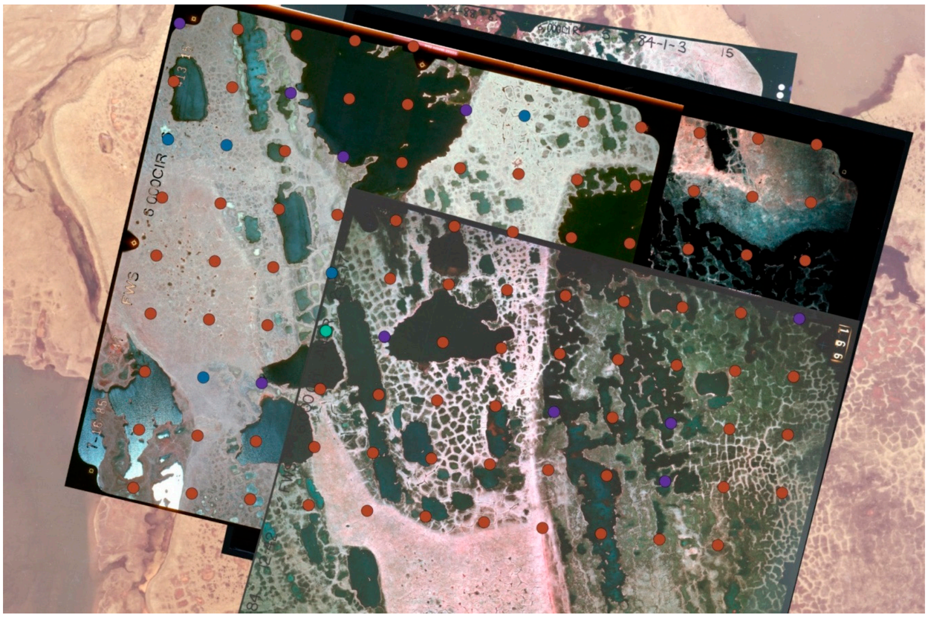

Figure 2. Example of a 100-point grid used for interpreting landscape change. Background is a 1981 aerial photograph, overlain with overlapping color-infrared (CIR) aerial photographs from 1984, 1985, and 1988. 1950 and 2003 images not shown. Site is on a thaw lake plain with polygonised microtopography in drained lake basins. Dots are grid points, 10-m-radius circles on the ground, color coded by type of change detected. Blue = ice-wedge degradation; purple = lake area increase; green = lake area decrease; brown = no change. Points are 160 m apart on the ground.

2.4. Image Interpretation

The stratified random sample had 5 sites in each of 7 ecoregions, with a systematic grid of 100 points per site. A grid approach was used instead of delineating polygons on each image because it was quicker. Image interpretation was done in ArcMap, with a separate file kept for detailed notes. At each point, a 10-m-radius circle was displayed on screen and the area inside the circle was visually evaluated on images. Satellite images were displayed in false-CIR and also in panchromatic for comparing to the 1950s-era black and white photographs.

We assigned landscape change types to each point based on differences detected within the circle between images from the three time periods. Change types were assigned for the early interval (~1952 to ~1982), recent interval (~1982 to ~2004), and overall. Vegetative and nonvegetative change types we detected are listed on Table A2. Differences were most often detected by a change in pattern or texture. We evaluated whether apparent changes were likely due to differences in image quality, including resolution, color scheme, or sun angle between years. Where image quality could not be confidently dismissed as the reason behind apparent change at a point, we did not record that point as changed. In practice, the only vegetative changes identified consistently were changes in density or size of trees, tall shrubs, and low shrubs, since dwarf shrubs and graminoid vegetation often lacked texture and potential changes between time periods could not always be identified. We overlaid historical fire perimeters mapped by the Alaska Fire Service on the images, but we found photointerpreted fire occurrence to be more reliable because burns were patchy within the perimeters and not all were mapped. We assigned the ice-wedge degradation change type in areas of polygonal microtopography but only at points where the width or depth of ice-wedge troughs changed between images. This was most often detected by changes in areal extent of water in troughs. Changes seen on the images but not at points were recorded in a separate file as incidental observations.

For each point in each time period, we recorded a number of variables. A vegetation type was assigned plus secondary vegetation types and water if they covered more than 10% of the circle.

Vegetation types were based on the Alaska Vegetation Classification [35] and are summarized in Table A1. To facilitate interpretation, the spectral and pattern characteristics of CIR images were described for each vegetation type, based on extensive previous work with aerial photographs. We also recorded presence or absence of ice-wedge polygon microtopography, polygon morphology (distinguishing high-, flat-, and low-centered polygons), and type of surface water (e.g., lake, river). To estimate the amount of water on the landscape, we recorded presence or absence of surface water at the center of each circle.

Vegetation data and photographs taken on the ground within 10–15 km of most grids in the Tundra Biome and in the lowlands of the Boreal Biome were available from previous projects. These reference data aided in interpretation of vegetation types on imagery. We did not visit grids on the ground but were able to fly over 22 of the 35 grids to make observations and take photographs that aided in interpretation. The main benefit was to verify photointerpreted burned areas by the presence of dead snags, which were often not distinguishable on imagery.

2.5. Environmental Variables

We compiled ancillary data on a suite of environmental variables, including climate, topography, geology, and fires. Data included mean annual and monthly temperatures for 1961–1990 from CRU6-9 (interpolated from climate station data, PRISM). Topographic variables were from the 2005 National Elevation Dataset. Geomorphic variables included general geologic unit, bedrock geology, geomorphology, and physiography derived from Jorgenson and Grunblatt [36]. We coded major rivers at each study site as glacially fed or nonglacial.

2.6. Data Analysis

Analysis involved data aggregation and summarizing of point data to produce descriptive statistics for regional and temporal comparisons. To simplify the analyses and increase sample sizes, we did several levels of aggregation including: (1) summarizing the frequency of each data category for each grid so that the grid (100 points) was considered the sample unit; (2) aggregating 29 image-interpreted change types into 19 broader categories (Table A2); (3) aggregating the seven ecoregions into three biomes (Table 1), and (4) simplifying time periods (e.g., 1947–1955) by assigning them the mean year of the period (e.g., ~1952). We lumped some change types into generally wetting change vs. generally drying change categories to enable assessment of broad hydrologic changes (Table A2). We also examined some environmental attributes to allow comparison of changes associated with specific factors, including (1) two types of substrate (alluvial and nonalluvial), (2) active floodplains of glacial vs. nonglacial rivers, and (3) four types of ice-wedge polygons.

To analyze changes, we calculated the mean frequency and confidence intervals for each change type and vegetation type within each ecoregion (original stratification). We them calculated the weighted mean for each biome (Tundra, Mountain, and Boreal) and the overall Refuge based on area of each ecoregion. For example, the Beaufort Sea Coast ecoregion was very small but had as many grids as the larger ecoregions, and data from this ecoregion were therefore given less weight. We calculated confidence intervals using a studentized bootstrap method with 10,000 replicates. For change types that were "opposites" (e.g., tree increase versus decrease) we also compared positive and negative changes to determine the net effect on a Refuge-wide scale. For comparing amount of change between the early and recent time intervals, which were of unequal duration, we calculated the annual rate of change (% of points changed/years in interval) for each grid in each time interval. Analyses were conducted in R (R Development Core Team, 2017).

3. Results

Analysis of time series of georeferenced aerial photos and satellite images at 35 sites in the Arctic National Wildlife Refuge revealed 29 types of landscape change over a 50-year period, which we simplified into 19 classes for analysis (Table A2). Below, we present the extent of change caused by the diverse geomorphic and ecological factors, first for the whole Refuge and then for the three major biomes of the Refuge, Tundra, Mountains, and Boreal. We highlight a few changes in particular biomes. We then compare rates of change between the early and recent intervals of the study. We also examine change types according to vegetation types and compare differences in change types associated with differing microtopography (polygonised vs. nonpolygonized) and substrate (alluvial vs. nonalluvial).

3.1. Change Types

Of all 3500 points we evaluated, 23% changed during the last half-century. Weighted by areal extent of each ecoregion, we estimated 18% of the Refuge changed (Table 3). The most common changes detected were wildfire and postfire succession (occurring on 6% of the Refuge), shrub increase (4%) or tree increase (2%) in the absence of fire, river erosion (3%) or deposition (2%), and thermokarst (soil ice-wedge degradation, 2%).

Change types varied by biome (Table 3, Figure 3). In the Tundra Biome, 19% of the area changed, mainly due to ice-wedge degradation (12%), river erosion or deposition (4%), and coastal changes (3%). In the Boreal Biome, 28% of the area changed, mainly due to fire and postfire vegetation succession (18%), tree and shrub increase in the absence of fire (7%), and landscape drying (2%). In the Mountain Biome, 10% changed, mainly due to river erosion and deposition (6%) overlapping with shrub increase in absence of fire (6%).

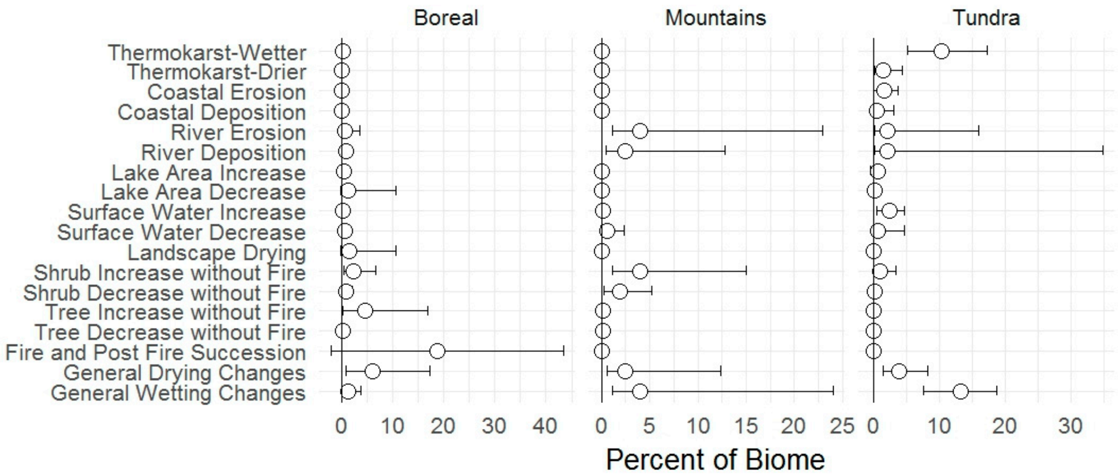

Figure 3. Percent of each biome with each major landscape change type, with means and 95% confidence intervals. Change types are defined in Table A2.

Because many types of change have opposing effects, we examined net change to evaluate the overall direction of landscape transitions over the study period (Figure 4). Based on weighted averages for the entire Refuge, tree and shrub increases were more common than decreases. This was mainly because fire was more prevalent before the study period began and gains associated with postfire successional recovery exceeded losses caused by fire. We estimate we could detect postfire vegetation succession after fires that had occurred up to ~50 years prior to our earliest imagery. Even in areas not affected by fire, we found small net increases in trees and shrubs indicating modest forest and shrubland expansion. Lakes and other surface water showed small net decreases, indicating more waterbodies shrank or were lost to drainage or water balance changes than increased in size. Ice-wedge degradation caused more ground wetting than drying and both coastal and river erosion caused more loss of land than was gained by deposition.

Table 3. Landscape changes detected on ~50-year time series of aerial images (between 1947 and 2007) in the Arctic National Wildlife Refuge, summarized by three biomes and seven ecological regions. Values are percentage of points that were affected (e.g., 45% of the Interior Lowlands points burned). Percentages for 7 ecological regions are based on 500 points per region. Percents for biomes and whole Arctic Refuge are weighted means, weighted by relative area of each ecoregion within its biome. Change types are described in Table A2.

Landscape Change	BIOMES										Whole Refuge
	Boreal			Mountains			North Slope Tundra				
	Interior Lowlands	Interior Uplands	Whole Biome	South Side	North Side	Whole Biome	Brooks Foothills	Coastal Plain	Coastal Marine	Whole Biome	
Fire & post-fire succession	45	11	18	0	0	0	0	0	0	0	6
Thermokarst wetting	1	0	<1	0	0	0	10	12	7	10	1
Thermokarst drying	<1	0	0	0	0	0	1	2	2	2	<1
Vegetation change without fire:											
Tree increase	4	5	5	<1	0	<1	0	0	0	0	2
Tree decrease	0	<1	<1	<1	0	<1	0	0	0	0	<1
Shrub increase	5	1	2	4	6	6	1	1	0	1	4
Shrub decrease	0	1	1	2	2	2	<1	0	0	<1	<1
River erosion	<1	1	1	4	4	4	1	4	1	2	3
River deposition	0	1	1	3	2	2	1	5	<1	2	2
Lake decrease	4	<1	1	0	0	0	0	<1	1	<1	<1
Lake increase	1	<1	<1	0	0	0	0	2	0	1	<1
Coastal erosion	0	0	0	0	0	0	0	0	18	2	<1
Coastal deposition	0	0	0	0	0	0	0	0	5	1	<1
Coastal storm surges & dunes	0	0	0	0	0	0	0	0	2	<1	<1
Landscape drying	2	1	2	0	0	0	0	0	0	0	<1
Glacial retreat	0	0	0	0	1	<1	0	0	0	0	<1
Scree slides	0	0	0	<1	<1	<1	0	0	0	0	<1
% with change of any type	58	20	28	9	11	10	14	24	36	19	18

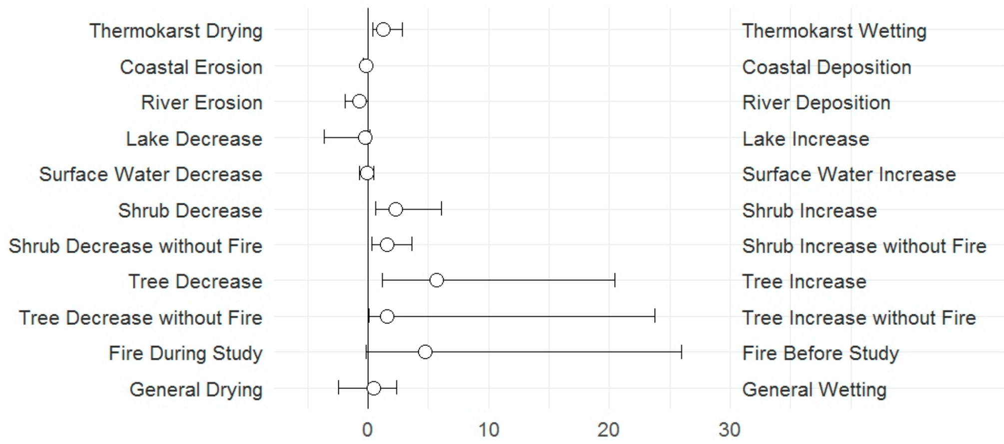

Figure 4. The net result of analyzing increase vs. decrease for opposing pairs of landscape change types. Values are mean percent, depicted as circles, with 95% confidence intervals given by error bars. Net increases are shown to the right of the zero line (y-axis), while net decreases fall to the left. Values shown indicate net change across the whole Refuge.

Rates of change were generally similar between the early and recent intervals (i.e., the first ~ 30 years compared to the last ~20 years) of the study. For some change types, there appeared to be a slight increase during the recent interval (Figure 5). These included ice-wedge degradation, tree and shrub increase in the absence of fire, general wetting, and general drying. However, the differences in net changes between intervals were small relative to the large variability encountered across the Refuge over the ~50-year study period.

Representative examples of imagery showing the changes associated with fire, increases in trees and shrubs, and ice-wedge degradation are shown in Figures 6–9. Other changes are illustrated in Figures A2–A5.

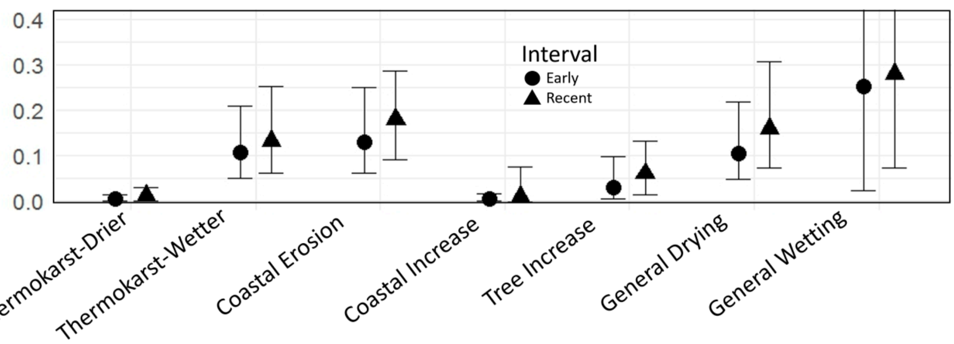

Figure 5. Annual rates of landscape change in the early study interval (1947–1955 to 1978–1988; circles) vs. the more recent interval (1978–1988 to 2000–2007; triangles), depicted for change types with differences between intervals. The y-axis is a mean annual rate of change (all < 1%/year), with 95% confidence intervals given by error bars.

3.2. Vegetation Types

Forest covered 19% of the Refuge, tall shrubs 5%, low or dwarf shrubs 28%, graminoid tundra 22%, and 26% of the Refuge had little or no vegetation (Table 4). Distributions of vegetation types were very different among the three biomes. Forest predominated in the Boreal Biome (52%), low and dwarf shrubs in the Mountain Biome (40%), and graminoids in the Tundra Biome (77%).

When examining types of change by vegetation type, we found forests had a high frequency of points that changed (39%), primarily due to wildfire and postfire vegetation succession. Tall shrubs showed the most change (44%) due to both wildfire and to riparian shrubs adjusting to river channel migration. Graminoid-dominated types changed less (16%), with ice-wedge degradation as the main cause.

3.3. Changes Associated with Alluvial and Polygonal Terrain

Alluvial terrain is dynamic due to channel migration, and polygonal terrain has abundant wedge ice that is sensitive to thermokarst associated with climate warming. We therefore compared changes occurring on alluvial vs. nonalluvial terrain and between high-, low, and flat-centered polygons to better understand potential drivers of change.

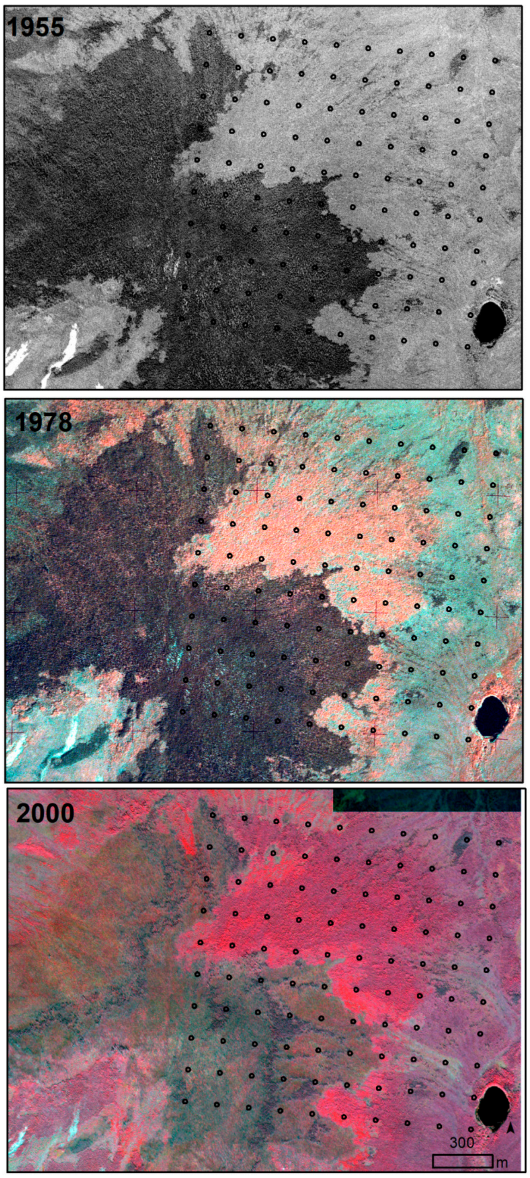

Figure 6. Time series showing a grid of 100 points with wildfire and postfire succession in the Boreal Biome. This forested site burned in 1950, leaving a patch of spruce forest (black in the 1955 and 1978 images). In 1986 most of the remaining forest disappeared in another fire that reached the site from the west and did not burn the dense young deciduous trees and shrubs to the east of the forest patch. Also visible are active layer detachment slides just SW of the grid (white streaks), probably caused by the 1950 fire. 2000 satellite image ©2018 DigitalGlobe, a Maxar company.

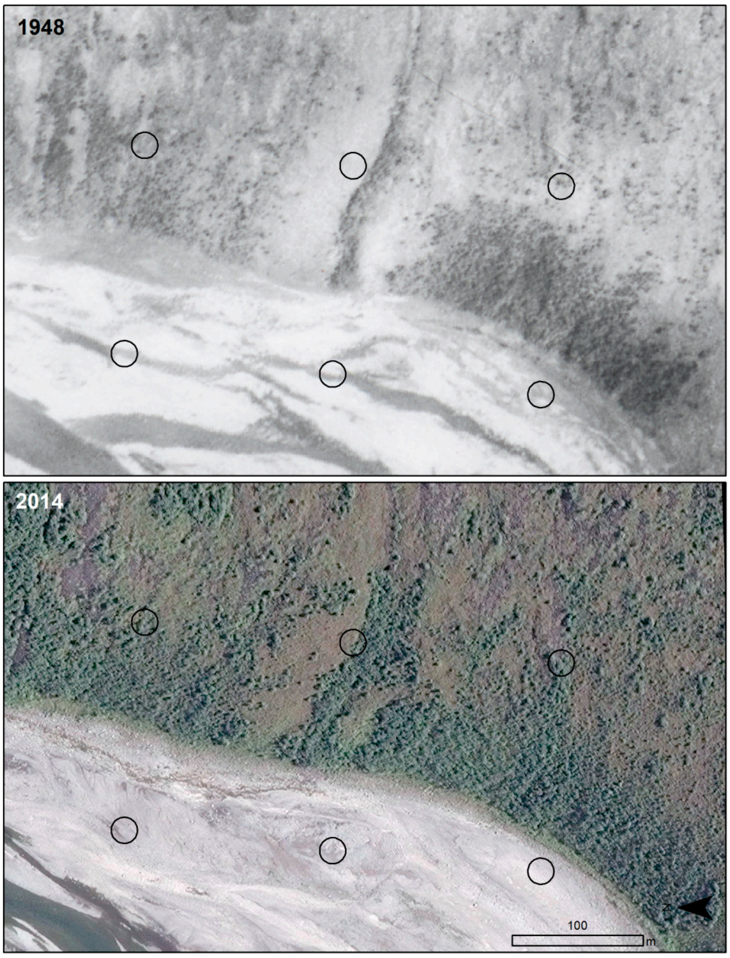

Figure 7. Images showing increase in alder shrub cover between 1948 and 2014 on a steep slope above a river in the northern Brooks Range, 30 km south of the north-most alder found to-date in the Arctic National Wildlife Refuge. 2014 satellite image ©2018 DigitalGlobe, a Maxar company.

River floodplains cover vast areas of the Refuge and have a gravelly, well-drained substrate that contrasts with the deeper organic soils found outside of floodplains. Of all study points, 23% were located on alluvial substrates, including active river floodplains, abandoned floodplains, and alluvial fans. Alluvial and nonalluvial substrates had a similar overall amount of change, but the vegetation and types of change were different. Alluvial substrates had more shrub-dominated area and less graminoid-dominated area. In particular, they lacked tussock tundra and had more tall shrubs.

On alluvium, the main changes over time were river erosion, deposition, and shrub increase or decrease. On nonalluvial substrates, the main changes were wildfire, tree increase, and ice-wedge degradation. The proportion of each grid that was alluvial varied greatly between grids, contributing greatly to the variability in our change-type data. Shrub changes were common on alluvial substrates, particularly shrub increase on alluvial fans in the mountains, and rare on nonalluvial (in absence of fire). Polygonization of the ground, requisite for the ice-wedge degradation change type, was almost absent on alluvium.

Because ice-wedge degradation was the major change type in the Tundra Biome and was only detected at points with visible polygonal surface patterns, we examined polygonized ground characteristics in more detail. Polygonized ground, indicative of a network of buried vertical ice wedges, varied among biomes. In the Tundra Biome, 67% of points had visible polygonal patterns, which were more common on flat ground than on slopes. Of these polygonised points, 64% were flat-centered, 17% low-centered, 9% high-centered, and 10% mixed. Most polygonized points were quite stable over time (Figure A2), with only 17% showing a change in ice-wedge degradation during the study period. In the other biomes, we found polygonized ground only in flat valley bottoms that were not on floodplains. Within the Interior Lowlands, 9% of points were polygonized but only a few had visible ice-wedge degradation, always after fire.

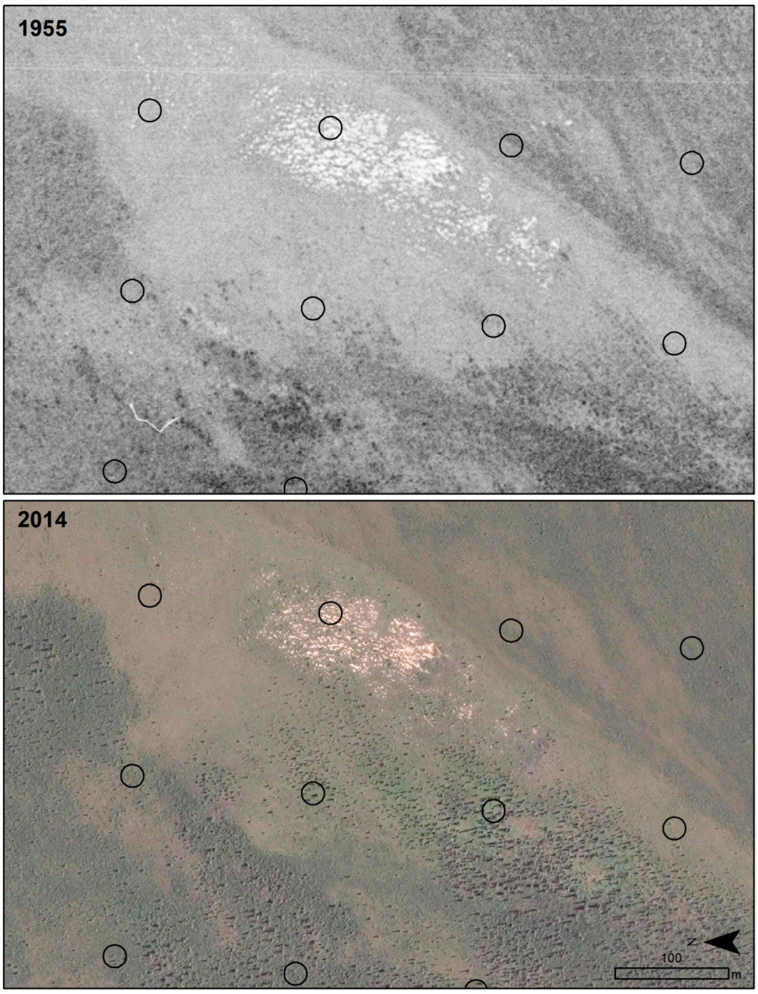

Figure 8. Images showing increase in tree cover at an upland site in the boreal forest between 1955 and 2014. 2014 satellite image ©2018 DigitalGlobe, a Maxar company.

The amount of polygonized ground differed by vegetation type. In the Tundra Biome, dwarf shrub tundra, moist sedge-Dryas tundra, and aquatic graminoid had the greatest proportion of polygonized points. In those types, plus moist sedge-willow and wet graminoid tundra, polygonized ground occurred at two-thirds or more of the points. For tussock tundra and saltmarsh vegetation, polygonized ground was observed at about half of the points. In the Boreal Biome, 27% of low shrub tundra points were polygonized. All other vegetation types had few or no polygonized points.

Ice-wedge degradation differed by polygon morphology and was more prevalent on points with flat-centered (22%) or mixed (high-, flat-, and low-centered; 23%) polygons than on points containing only low-centered (13%) or only high-centered (5%) polygons. Flat-centered polygon points initially had little vertical relief compared to points with low- or high-centered polygons; but at some of these points, ice-wedge troughs deepened over time, forming pools at trough intersections. This was most noticeable on points with moist sedge-Dryas tundra (Figure 9), likely due to soil properties associated with that vegetation type. (Specifically, high ground- ice contents, and deep summer thaw associated with frost boils that have bare mineral soil without an insulating organic layer.) Points with mixed polygons were probably unstable because of the ongoing ice-wedge degradation that had caused their mixed morphology. Points with low-centered polygons (most common in salt marshes and drained lake basins on thaw lake plains) were surprisingly stable over the half-century study period. Points with high-centered polygons were uncommon and also quite stable. High-centered polygons appeared to generally be the "changed" feature that remained following degradation. These points often had shrubby vegetation, which may have shaded the soil and minimized further thaw.

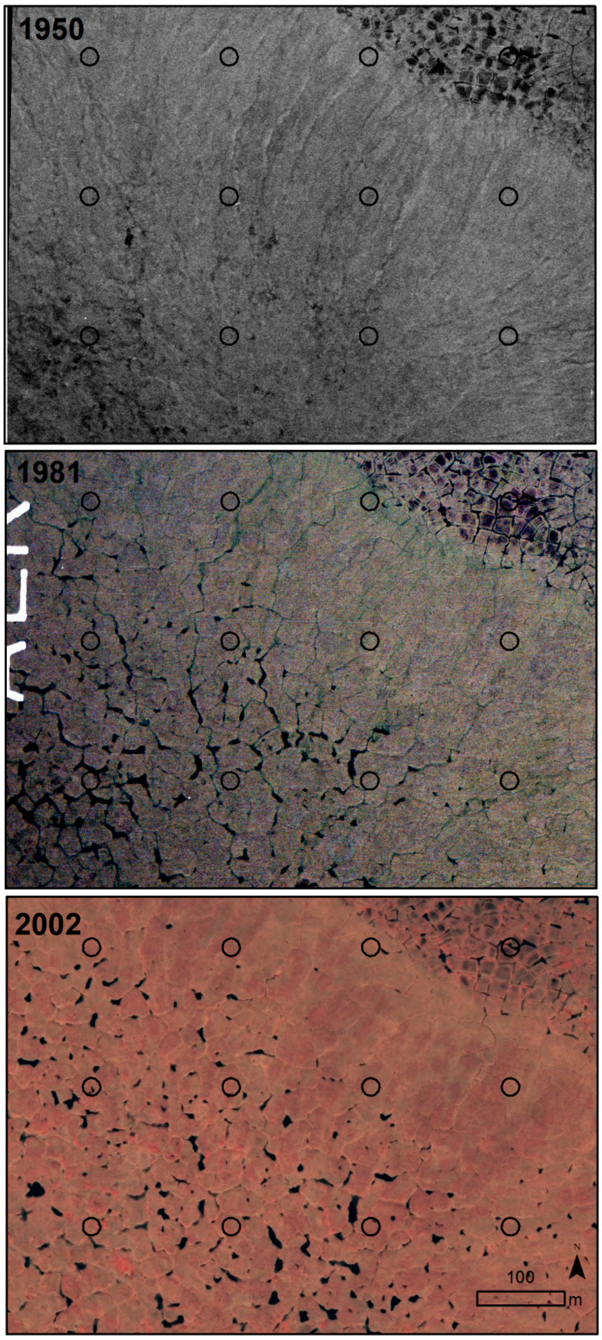

Figure 9. Time series of images showing ice-wedge degradation, evidenced by enlarged troughs and increased surface water on flat-centered polygons in a tundra basin and on an adjacent gentle slope. Note the lesser change visible in the wet, low-centered polygons (upper right). 27% of points at site had a change in ice-wedge degradation over the study period. 2002 satellite image ©2018 DigitalGlobe, a Maxar company.

Table 4. Distribution of vegetation types in the Arctic National Wildlife Refuge and in each of the three biomes, most common type of change detected in each vegetation type, and percent of points with each change type. Vegetation types are described in Table A1.

Vegetation Types	% of Whole Arctic Refuge	% of Tundra Biome	% of Mountain Biome	% of Boreal Biome	Most Common Change Detected in This Vegetation Type	% with Any Change
FOREST	19	0	2	52	Fire & post-fire succession	39
Spruce Forest	9	0	2	21	Fire & post-fire succession	31
Mixed Forest	8	0	0	25	Fire & post-fire succession	39
Broadleaf Forest	2	0	0	6	Fire & post-fire succession	77
TALL SHRUB	5	0	5	9	Shrub increase, with or without fire	44
Tall Riparian Shrub	2	0	3	1	River erosion & shrub increase (without fire)	53
Tall Non-riparian Shrub	3	0	2	8	Fire & post-fire succession	38
LOW OR DWARF SHRUB	28	12	40	21	Fire & post-fire succession	19
Low Riparian Shrub	3	1	4	1	River erosion	32
Low Non-riparian Shrub	14	10	15	20	Fire & post-fire succession	26
Dwarf Shrub	11	1	21	<1	Shrub increase (without fire)	7
GRAMINOID	22	77	9	15	Thermokarst-wetting	16
Tussock Tundra	6	19	4	4	Thermokarst-wetting	5
Moist Sedge-Dryas Tundra	6	25	2	3	Thermokarst-wetting	24
Moist Sedge-Willow Tundra	4	15	2	3	Thermokarst-wetting	14
Wet Graminoid Tundra	5	15	1	7	Thermokarst-wetting	16
Salt marsh and Aquatic	<1	3	0	<1	Thermokarst-wetting & coastal erosion	27
OTHER	26	11	43	3	River erosion & deposition	20
Sparsely Vegetated	6	1	11	<1	Shrub increase (without fire)	15
Non-vegetated	17	4	31	3	River erosion	19
Water	3	6	1	1	River deposition	21

4. Discussion

The Arctic National Wildlife Refuge has heterogenous landscapes with diverse ecosystems that are subject to a wide variety of geomorphic and vegetation processes that drive change. During the ~50-year study period, 18% of the Refuge underwent some type of landscape change, primarily due to wildfire, postfire succession, changes in shrub and tree cover, river dynamics, and ice-wedge degradation. This is similar to the amount of change detected in the Arctic Network of National Parks, located to the west of the Refuge, where a similar methodology found 24% of 206 systematically distributed plots showed change between 1975–1985 and 2008–2010 [27]. Our finding also compare to an Alaska-wide analysis, in which Pastick et al. [37] found 14% of the landscape had undergone change from 1984 to 2015, based on an analysis of spectral trends in Landsat imagery.

Below, we discuss some of the dominant changes affecting the landscape, compare and contrast the major drivers of change across the Refuge, evaluate rates of change during early and recent time intervals, and discuss the limitations of our remote sensing approach.

4.1. Change Types

We documented 19 broad categories of change associated with geomorphic and ecological processes. The major change types that emerged as most prevalent on the Refuge landscape included fire, river channel dynamics, tree or shrub increase, ice-wedge degradation, changes to the coastline, and hydrologic changes that included lake expansion and drainage, discussed in more detail below.

Wildfire caused the most change in our study Refuge-wide (6%) and was an important driver of change in the Boreal Biome (18%). Wildfire is a natural part of the boreal forest ecosystem (Figure A6). While fire frequency has increased in recent decades in Alaska [38], in the Refuge a huge area that burned in 1950 has been unequaled by any subsequent year. Therefore, large areas have been recovering from that fire, and our study found more tree increase than decrease after wildfire. Fire occurred only at our forested grids. Fires are known to occur in the tundra of northern Alaska but are uncommon [39]. The recent large fire near the Anaktuvuk River, visible on Figure A6, indicates that fire activity within the Tundra Biome could increase with climate warming, which could exacerbate thermokarst [40,41]. Severe fires accelerate thermokarst by removing the insulating soil organic layer, allowing summer heat to penetrate and thaw the permafrost [42]. We found some evidence that this process has occurred within the Refuge, as we noted several active-layer detachment slides that began within five years after fires (Figures 6 and A5).

Channel dynamics of active river floodplains can result in rapid changes. Half of our grids included points on active floodplains and we found river erosion and deposition were important drivers of change, affecting 5% of the Refuge. Differences between erosion and deposition can be linked to the rapid melting of glaciers in the Brooks Range [43]. The glacially fed river floodplains had twice the frequency of changed points as the nonglacial river floodplains (63% vs. 30% of active floodplain area), including more erosion, deposition, and shrub increase or decrease. The ratio of river erosion to deposition was skewed slightly towards erosion on the glacial rivers, and towards deposition on the nonglacial.

Shrub expansion onto tundra is widespread in the Arctic, with large ramifications for ecological processes and climate feedbacks [44]. In the Refuge, shrub cover increase in the absence of fire occurred almost entirely in the Mountain and Boreal Biomes, on alluvial substrates (e.g., active or abandoned floodplains, banks along floodplains, or alluvial fans). This change type affected 4% of the Refuge. In comparison, Swanson [45] photointerpreted tall shrub presence and density at 471 plots (mostly Mountain Biome) in the Arctic Network of National Parks and found that 8% had dense canopies of tall shrubs (often on floodplains), associated with higher summer temperatures, deep summer thaw, and well-drained soils. Tape et al. [46] also observed widespread shrub expansion on floodplains or nearby slopes. The scarceness of shrub increase we detected in the Tundra Biome and on nonalluvial surfaces throughout the Refuge appeared to be linked to soil conditions, and perhaps also to seasonality. Peak solar radiation at these latitudes occurs in late June, at which time soils may be thawed in Brooks Range valleys, especially on well-drained alluvial substrates, allowing plants to begin growth. The Tundra Biome, narrower within the Arctic Refuge than elsewhere in Arctic Alaska, is more affected by colder temperatures nearer to the Arctic Ocean. This causes soils to remain frozen near the ground surface at summer solstice, retarding the ability of shrubs to take full advantage of that period of maximum solar radiation.

Tree increase unrelated to fire was found almost entirely in the Boreal Biome (5%). One Boreal grid showed altitudinal tree line advance, where spruce trees had advanced out of gullies and onto high tundra between the earliest and latest time series images (Figure 8). Overflights of this grid together with a hand-drawn map showing tree extent in 1911 [47] indicate that the advance was not due to vegetation recovery following wildfire. At another grid on an inactive floodplain trees had become denser in wetlands, perhaps attributable to reduced flooding. The overall increase in tree cover was greater in the recent interval than in the early one. Little tree increase occurred at other grids (without wildfire). A review of worldwide tree line studies found that only 52% of sites showed tree line advance [48].

Ice-wedge degradation (a thermokarst process) is affecting ecosystems throughout the Arctic [21,49]. It affected 2% of the entire Refuge and was the dominant change detected in the Tundra Biome (12%). In comparison, ice-wedge degradation was observed at a few of 206 photointerpreted plots in the Arctic Network of National Parks [50]. Within small, targeted areas in northern Alaska, the extent of ice-wedge degradation increased from 0.5% to 4.4% (1945–2001) near Fish Creek [21] and increased from 0.9% to 7.5% (1949–2012) near Prudhoe Bay [30]. Farquharson et al. [51] found thermokarst troughs and pits covered 7% of 12 small mapped areas across northern Alaska. For central and northern Alaska, Jorgenson et al. [52] found thermokarst features occurred on 8% of sample points on airphotos from 2005 and 2006, with the frequency of occurrence much higher in the continuous permafrost zone in arctic Alaska (13.5%) compared to the discontinuous zone in boreal Alaska (5%). Ice-wedge degradation usually causes radical redistribution of water, resulting in newly wetting or drying conditions [53]. The only type of thermokarst recorded in our study was ice-wedge degradation, which overall caused much more wetting (1.5%) than drying (0.2%). Other types of thermokarst may be common in the Refuge, going undetected in our study due to small areal extent. For example, several small active-layer-detachment slides (ALDs) were incidentally observed to have occurred at one forested site after a wildfire, although not at a point (Figure 6). Many slides up to 90-m long have also occurred in severely burned forest 2 km NW of another study site (Figure A5). In comparison, 848 ALDs and 276 retrogressive thaw slumps were mapped within the 2.7 million hectare Noatak National Preserve [54].

On the Beaufort Sea coast, there were changes associated with coastal erosion, deposition, and salt water intrusion during storm surges. Deposition occurred at the mouths of rivers, and elsewhere the shore eroded gradually, seldom more than 1 m/year. Jorgenson and Brown [55] compiled mean annual erosion rates (1950s to 1980s) for sections of Refuge's coastline, and found coastline changes that ranged from erosion at ~1 m/year to accretion at ~12 m/year. Rates depended on the coastline type and soil texture. A long-term monitoring site in the Refuge had a mean annual erosion rate of 0.5 m/year between 1949 and 2001 [56]. In comparison, Jones et al. [57] documented a maximum erosion rate of 18.3 m/year at a point north of Teshepuk Lake, in low-lying thaw lake terrain that is rare within the Refuge.

Hydrologic changes included changes in lake area, river channel migration, irregular surface water changes on vegetated ground, water redistribution associated with ice-wedge degradation, and surface drying on inactive floodplains. Changes in the Tundra Biome tended to be related to landscape wetting (mainly ice-wedge degradation and surface water increase), while changes in the Boreal Biome tended to involve landscape drying (including reduced area of lakes and recent wildfire). Lake area tended to increase in the Tundra Biome and decrease in the Boreal Biome, where we found the process of lake drying on inactive floodplains left concentric rings of shrub and graminoid vegetation in former lake beds. Our results are consistent with those of Riordan et al. [24], who examined surface water, lakes, and ponds at 11 regions of Alaska, using images from the 1950s to 2002. They found a decrease in the area of closed-basin ponds in all locations except the Arctic coastal plain. In the adjacent Yukon Flats National Wildlife Refuge, historic aerial imagery indicates that lake drying and vegetation invasion have occurred in the Boreal Biome since about the 1980s [58]. Necsoiu et al. [59] mapped waterbodies on a time series of high-resolution imagery for the Kobuk Valley and found total surface area decreased by only 0.4% during 1951–1978, but then decreased by 5.5% during 1978–2005. In contrast, Plug et al. [60] used a time series of Landsat imagery (1978–2001) to show that lakes mostly increased during 1978–1992 and decreased during 1992–2001. Our limited sampling did not detect the decline in river icings documented by Pavelskiy et al. [61].

4.2. Vegetation Types

Although only 18% of the Refuge changed during the study period, some vegetation types had much higher amounts of change. Tall shrub and broadleaf forest together covered just 7% of the Refuge, but when present, changed greatly (38% and 77% of points, respectively). These types were usually associated with early to mid-succession stages after fire or on dynamic river floodplains. In contrast, only 7% of points changed in dwarf shrub vegetation. It was the most common vegetation type in the Mountain Biome, covering high-elevation, dry, rocky slopes that were not prone to any of the change types we detected. Only 5% of tussock tundra points changed, the least of all tundra types, likely because it occurred mainly on slopes in the Arctic Foothills, where water was less likely to impound and cause ice-wedge degradation than on the flatter Coastal Plain.

4.3. Rates of Change

We found little evidence for increasing rates of change over the course of our study, even though the recent interval of the study coincided with a period of increased climate warming in northern Alaska. An apparent slight increase in rates of change for ice-wedge degradation, surface water increase, and tree increase in absence of fire suggested a response to a warming climate, but the variability in change observed among grids was too high to detect a difference (Figure 5). The small differences in rates of change were unexpected, given that there was a large jump in air temperatures after a large Pacific Decadal Oscillation (PDO) shift in 1977 [4].

4.4. Limitations and Applications of Remotely Sensed Change

There were some limitations on our ability to detect change related to image quality and high spatial variability. We chose to manually interpret the changes we could see on images, using visual cues, such as pattern, texture, brightness, and juxtaposition, as well as ecological knowledge of the interpreters. When imagery was high quality, this worked very well and proceeded rapidly. The aerial photographs varied in quality and resolution, however. In the Mountain Biome, some of the oldest photographs in the southern Brooks Range were of poor quality. In addition, the aerial photographs were difficult to rectify on mountain slopes due to steepness and to lack of reliable ground reference points on slopes that had only scree and dwarf shrub vegetation. We believe we are correct in concluding that there was little change in the Mountain Biome other than on river floodplains, despite the image limitations. Images for the Boreal Biome were generally acceptable and changes in forested types were easy to detect. Imagery was excellent for the Tundra Biome but we likely could not detect subtle vegetation changes since most plants are <0.3 m tall and are hard to differentiate on imagery, partly due to lack of shadows. We could not reliably detect increases in dwarf shrubs, but if taller shrubs (e.g., alder) were to invade the tundra, they would be easy to detect. A vegetation type was assigned for each time period, but in practice, types could not be photointerpreted on the 1950s images without referring to the later images, so we did not analyze changes in vegetation type over the study period. Stereoscopy could have improved interpretation but was not used.

The combination of high variability in landscape characteristics (e.g., the diverse vegetation types and substrates) and high variability in drivers of change across the Refuge landscape, combined with a small sample size (35 sites spread across three biomes), limited our ability to detect significant differences in the data. In particular, large differences in the abundance of highly dynamic alluvial terrain, polygonized ground that is subject to ice-wedge degradation, and fires that are highly variable in space and time lead to high variability in both vegetation and change types. Due to high between-site variability and low number of sites, confidence intervals overlapped for most of the comparisons we made. As high-resolution satellite imagery becomes more available, cost decreases, and methods are developed to efficiently automate the image rectification process, larger sample sizes will be feasible. Similar studies to ours could have larger sample sizes with little increase in interpretation effort by having more sites and fewer points per site. Yet, the high variability among sites related to different vegetation types being affected by different change drivers in different regions at different times will remain a large obstacle in assessing whether changes are significant.

The 15 grids in the Tundra Biome had the best-quality aerial photographs, so we are most confident of our results for that biome. The photographs from the first time period (~1952) were of better resolution and higher quality than those available for the rest of the Refuge. For the second time period (~1982), most Tundra grids had excellent aerial photographs from four years: 1981, 1984, 1985, and 1988. We used the 1985 photograph to record data for that time period. However, we eventually georeferenced and examined the other photos at most grids to aid in interpretation. This was useful for detecting ice-wedge degradation because it gave us a range of different water levels to determine what normal seasonal variability was (Figure A2). We found observed widths and extent of ice-wedge polygon troughs remained fairly constant for the 1981–1988 period despite expected rising and falling water levels over the summer season, allowing more confidence in our interpretation of ice-wedge degradation. We believe this is because actively subsiding troughs are steep sided, minimizing changes to the aerial extent of water as water rises and lowers in the troughs. We were conservative about assigning ice-wedge degradation change. For example, if a point had similar patterns of surface water in ~2004 to any one of the 1980s years, we did not interpret it as changed, even if the area of surface water was different than in 1985.

These empirical data can be applied to modelling efforts to improve prediction of future change by providing realistic input variables to models. The dataset developed by this study has been used for projecting future changes across a broader region of northern Alaska using state-transition modeling [62] and for landscape change analysis using satellite remote sensing and decision-tree modeling [37]. We found that environmental variables were very useful in explaining variations in change types across the region and can be incorporated into other studies. Sormunen et al. [63] showed that including local environmental conditions, such as topography and soils information, in models of subarctic vegetation change greatly improved the predictive accuracy and changed the model outputs by constraining possible vegetation shifts using more realistic data. They found that climate-only models overestimated the amount of vegetation change. Results including environmental data fine-tuned the predictions and could also predict potential refugia in future climates. Our findings of the large differences between change types on alluvial vs. nonalluvial substrates, such as shrub changes on alluvial and ice-wedge degradation on nonalluvial terrain, can be used to improve modelling of future landscape changes with climate change.

5. Conclusions

Manual interpretation of time series of historical aerial photographs and satellite images in the Arctic National Wildlife Refuge of Alaska showed that 18% of the Refuge had detectable landscape changes over a half-century. Wildfire was the most common change agent, resulting in extensive post-fire successional vegetation changes in forested parts of the Refuge. Other common changes were tree or shrub increase without fire, river erosion and deposition, and ice-wedge degradation. The change types varied greatly among biomes, with ice-wedge degradation occurring mainly in the Tundra Biome, shrub increase and river changes in the Mountain Biome, and fire and postfire succession in the Boreal Biome. When change types were examined as generally wetting change vs. generally drying change, the Tundra Biome tended to be affected by landscape wetting (mainly ice-wedge degradation), while the Boreal biome tended to be affected by landscape drying (including fire, reduced area of lakes, and land surface drying). The recent interval of our study period (1980s to 2000s) coincided with a documented shift towards a warmer climate; this interval had slightly more change in several categories, including ice-wedge degradation, lake changes, and tree and shrub increase. However, differences in the amount of change were not statistically significant, given the high variability of changes across the heterogeneous landscapes.

Our unbiased stratified random sampling design allowed extrapolation of the results to the whole Refuge, which is not possible with the more common approach of focusing studies in areas with known, dramatic changes. Results of this study can be incorporated into models to predict changes and outcomes for future climate-warming scenarios in the Arctic. This study can be repeated in the future to continue tracking changes occurring across this diverse landscape during a time of rapid climate warming. Much of the Arctic is remote and roadless, so monitoring landscapes using high-resolution imagery can be the most cost effective approach. It will become even more feasible in the future, as increasing availability of multispectral, high-resolution satellite imagery will provide more and shorter time intervals that will improve monitoring and detection of trends.

Author Contributions: Conceptualization, J.C.J. and M.T.J.; Methodology, M.T.J.; Formal Analysis, K.M.O. and J.C.J.; Investigation, J.C.J. and M.L.B.; Data Curation, K.M.O. and J.C.J.; Writing-Original Draft Preparation, J.C.J.; Writing-Review & Editing, M.T.J., M.L.B. and K.M.O.; Visualization, K.M.O. and J.C.J.

Funding: This research was funded by the U. S. Fish and Wildlife Service.

Acknowledgments: We thank Alan Brackney for GIS support, Cashell Villa and Nicole Grant-Hoffman for help georeferencing aerial photographs and McCrae Cobb for statistical help. We also thank Bill Manley, LeAnn Lestak and Dorte Dissing for training in image rectification, interpretation and database design. Anonymous reviewers provided useful comments. Digital Globe Inc. gave permission to use satellite images in the figures. The findings and conclusions in this article are those of the authors and do not necessarily represent the views of the U.S. Fish and Wildlife Service.

Conflicts of Interest: The authors declare no conflict of interest.

Appendix A

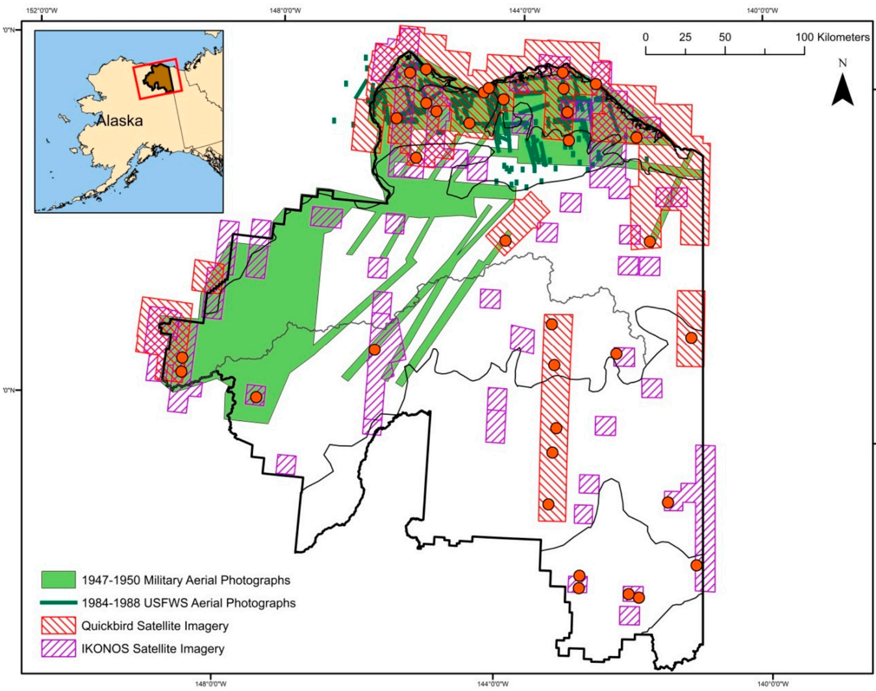

Figure A1. Map of available imagery for landscape change detection project. For 1947–1950 photos, green shows general area of coverage but not individual flight lines; gaps occurred between lines.

Table A1. Vegetation types of the Arctic Refuge based on the Alaska Vegetation Classification [35].

Vegetation Type	Description
1 FOREST	Trees >10% cover. Includes all trees even if temporarily low stature due to intermediate succession after fire or flooding. Includes open and closed canopy forest and woodlands. Understory has abundant shrubs, forbs, mosses and lichens.
1.1 Spruce Forest	>60% of tree cover is needleleaf trees, mainly *Picea glauca* and also *Picea mariana* in most southern areas
1.2 Mixed Forest	40–60% each of spruce and broadleaf trees
1.3 Broadleaf Forest	>60% of tree cover is broadleaf. Poplar (*Populus balsamifera*) mainly on floodplains, aspen (*Populus tremuloides*) and paper birch (*Betula neoalaskana*) mainly after fire.
2 TALL SHRUB	Shrubs >1.5 m tall cover >25% of area. Includes open and closed canopies. Willows, mainly *Salix alaxensis*, and alder (*Alnus viridis*).
2.1 Tall Riparian Shrub	Tall shrubs on river floodplains, banks of floodplains and narrow drainages.
2.2 Tall Non-riparian Shrub	Non-floodplain, common in early and intermediate stages of post-fire succession
3 LOW OR DWARF SHRUB	Shrubs <1.5 m tall cover >25% of area.
3.1 Low Riparian Shrub	Shrubs 20–150 cm tall on river floodplains, banks of floodplains and narrow drainages. Mainly willows, e.g., *Salix pulchra*, *S. richardsonii*.
3.2 Low Non-riparian Shrub	Shrubs 20–150 cm tall not on floodplains. Mainly the same willows above plus shrub birch (*Betula glandulosa, B. nana*) and other willows, e.g., *S. glauca*.
3.3 Dwarf Shrub	Shrubs <20 cm tall. Mainly mountain avens (*Dryas* species, mainly *D. integrifolia*), dwarf willows (e.g., *Salix reticulata*), blueberry (*Vaccinium uliginosum*), cranberry (*V. vitis-ideae*), Labrador tea (*Ledum groenlandicum*, *L. decumbens*). On mountain slopes, late snow-melt areas, high-centered polygons and infrequently flooded river terraces. Many additional species in alpine areas.
4 GRAMINOID	Graminoids predominate. The first 3 below also have high cover of mosses and dwarf and low shrubs.
4.1 Tussock Tundra	Dominated by the tussock-forming sedge *Eriophorum vaginatum*. Includes shrubby tussock tundra, which may have >25% low shrub cover.
4.2 Moist Sedge-Dryas Tundra	Dominated by sedges, usually *Carex bigelowii*, and the dwarf shrub *Dryas integrifolia*
4.3 Moist Sedge-Willow Tundra	Dominated by sedges, usually *Carex aquatilis* and *Eriophorum angustifolium*, and willows, usually *Salix pulchra*.
4.4 Wet Graminoid Tundra	Sedges, usually *Carex aquatilis* and *Eriophorum angustifolium*. Soil saturated throughout the growing season, so little willow or moss cover, except aquatic mosses. Some grass-dominated near the coast, e.g., *Dupontia fisherii*.
4.5 Aquatic graminoid	Sedges and grasses in persistent standing water, mainly in shallow lakes
4.6 Salt marsh	Coastal marshes with salt-tolerant species, mainly *Carex subspathacea*, *Puccinellia* spp. and *Dupontia fisherii*
5 OTHER	Little cover of live plants, mainly on steep mountain slopes and active floodplains
5.1 Sparsely Vegetated	10–30% cover of vegetation
5.2 Non-vegetated	0–10% vegetation
5.3 Water	<10% vegetation

Table A2. Twenty-nine types of landscape change detected on time series of aerial images in the Arctic Refuge with descriptions, 19 broad change types, and the number of points in each type.

Interpreted Change Type	Broad Change Type	Definition of Interpreted Type	# Points
1 Fire:		Any change due to wildfire, even if the fire occurred before the study period	
1.1 Fire & post-fire succession	Fire & post-fire succession	Burned by wildfire, causing vegetation changes	273
1.2 Fire, post-fire & thermokarst	Fire & post-fire succession	Burned, causing vegetation changes and ice wedge melting	5
2 Ice-wedge degradation (Thermokarst):		Included only points with a change from one time period to the next, not all points with polygonal microtopography. Recorded for saltmarsh vs. other.	
2.1 Thermokarst-wetter	Thermokarst-wetter	Thermokarst with wetting effects within the circle. Increase in depth, width, or extent of ice-wedge polygon troughs, often with increase in water in troughs.	130
2.2 Thermokarst-drier	Thermokarst-drier	Thermokarst with drying effects within the circle. Drying of troughs above ice wedges due to increased drainage of the general area as troughs enlarged, became more connected and allowed drainage. Or, graminoid cover increasing in troughs, accumulating dead leaves and causing less area and depth of surface water. Or, drying of polygon centers.	22
3 River changes:			
3.1 River bank erosion	River erosion	Erosion into bank or uplands	11
3.2 River erosion	River erosion	More river water in circle than in previous time period. River channel moving around on active floodplain, not into uplands.	62
3.3 River deposition	River deposition	Less river water in circle than in previous time period. River channel moving around on active floodplain.	61
4 Lake changes:		Recorded only if change in surface water detected within the 20-meter circle, not at points in centers of lakes	
4.1 Lake drying	Lake decrease	Lake became smaller and shallower. Water in circle disappeared.	20
4.2 Lake drained	Lake decrease	Lake evidently drained all at once	5
4.3 Lake accretion	Lake decrease	Sediment accreted along edge of lake, so less open water in circle	1
4.4 Lake erosion	Lake increase	Lake eroded bank inside the circle, so more open water in circle	9
4.5 Lake increase	Lake increase	Lake became larger. In circle, water covered previous land.	5
5 Vegetation changes:		Recorded separately for post-fire changes vs. non-fire-related	
5.1 Shrub decrease	Shrub decrease	Decreased cover of shrubs	26
5.2 Shrub increase	Shrub increase	Increased cover of shrubs	83
5.3 Tree decrease	Tree decrease	Decreased cover of trees	2
5.4 Tree increase	Tree increase	Increased cover of trees	47

Table A2. *Cont.*

Interpreted Change Type	Broad Change Type	Definition of Interpreted Type	# Points
6 Coastal changes:			
6.1 Barrier erosion	Coastal erosion	Decreased area of off-shore barrier island in circle	4
6.2 Coastal erosion	Coastal erosion	Erosion not including delta mud flat changes	43
6.3 Salt marsh flooded	Coastal erosion	Within a salt marsh, increase in area of water and decrease in land in the circle	2
6.4 Delta erosion	Coastal erosion	Decreased area of delta mud flats in circle (and increased area of sea)	20
6.5 Barrier deposition	Coastal deposition	Increased area of barrier island in circle	5
6.6 Coastal deposition	Coastal deposition	Deposition not including delta mud flats	2
6.7 Delta deposition	Coastal deposition	Increased area of delta mud flats in circle	10
6.8 Deposition in creek	Coastal deposition	Storm surge pushed beach gravels & logs into mouth of creek, forming pond	1
6.9 Drift line move	Coastal - other	Driftwood line moved further inland over time, reaching to or beyond the point, indicating salt water intrusion	4
6.10 Salt killed tundra	Coastal - other	Dead tundra vegetation, killed by salt water intrusion	1
6.11 Sand deposition	Coastal - other	Sand deposition onto tundra from beach during storm surge	1
6.12 Sand dune change	Coastal - other	Movement of sand dunes caused change in vegetation and sand cover	5
7 Surface water change:			
7.1 Surface water increase	Surface water increase	Surface water, recorded at center of circle, absent in first year and present in last year	45
7.2 Surface water decrease	Surface water decrease	Surface water, recorded at center of circle, present in first year and absent in last year	22
8 Other:			
8.1 Land surface drying	Land surface drying	Drying of land surface, usually on abandoned floodplains near drying lake basins	16
8.2 Scree fan increase	Scree fan increase	Scree at base of steep slope spread out over previously vegetated area	2
8.3 Glacial retreat	Glacial retreat	Points on glacier in first 2 time periods and on bedrock outcrops protruding through the thinning glacier in last time period	3
9. General drying or wetting:		Composite categories derived from some of the change types recorded	
9.1 General drying changes	General drying changes	Sum of points with drying changes: Less water at surface due to river deposition, lake or surface water decrease, thermokarst with drying, land surface drying or wildfire during the study period	182
9.2 General wetting changes	General wetting changes	Sum of points with wetting changes: More water at surface due to river erosion, lake or surface water increase, or thermokarst with wetting	236

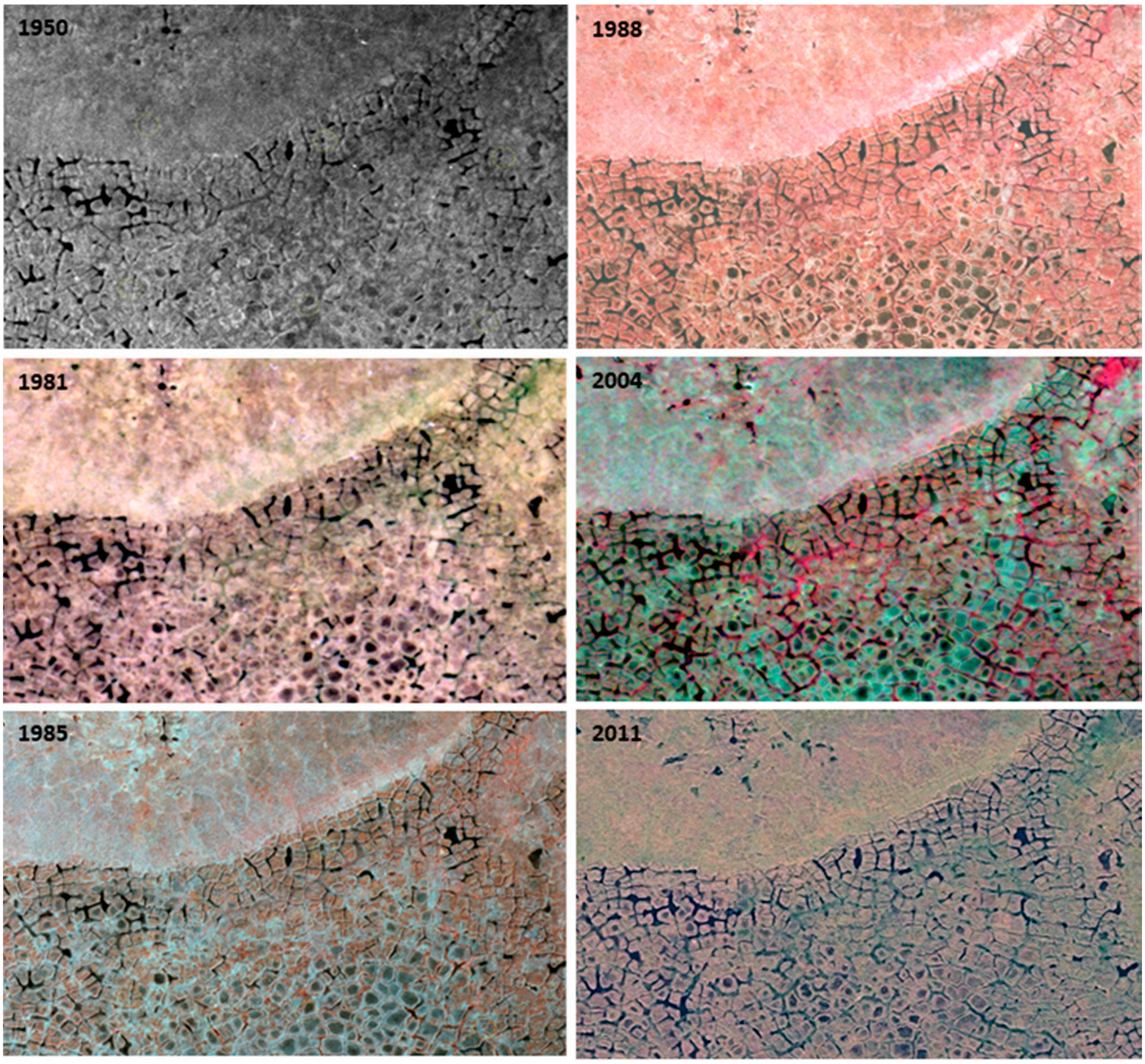

Figure A2. Time series of six images over a 61-year period on coastal plain tundra with flat-centered polygon morphology. Some change occurred, but there was overall surprising stability. 2004 and 2011 are satellite images ©2018 DigitalGlobe, a Maxar company.

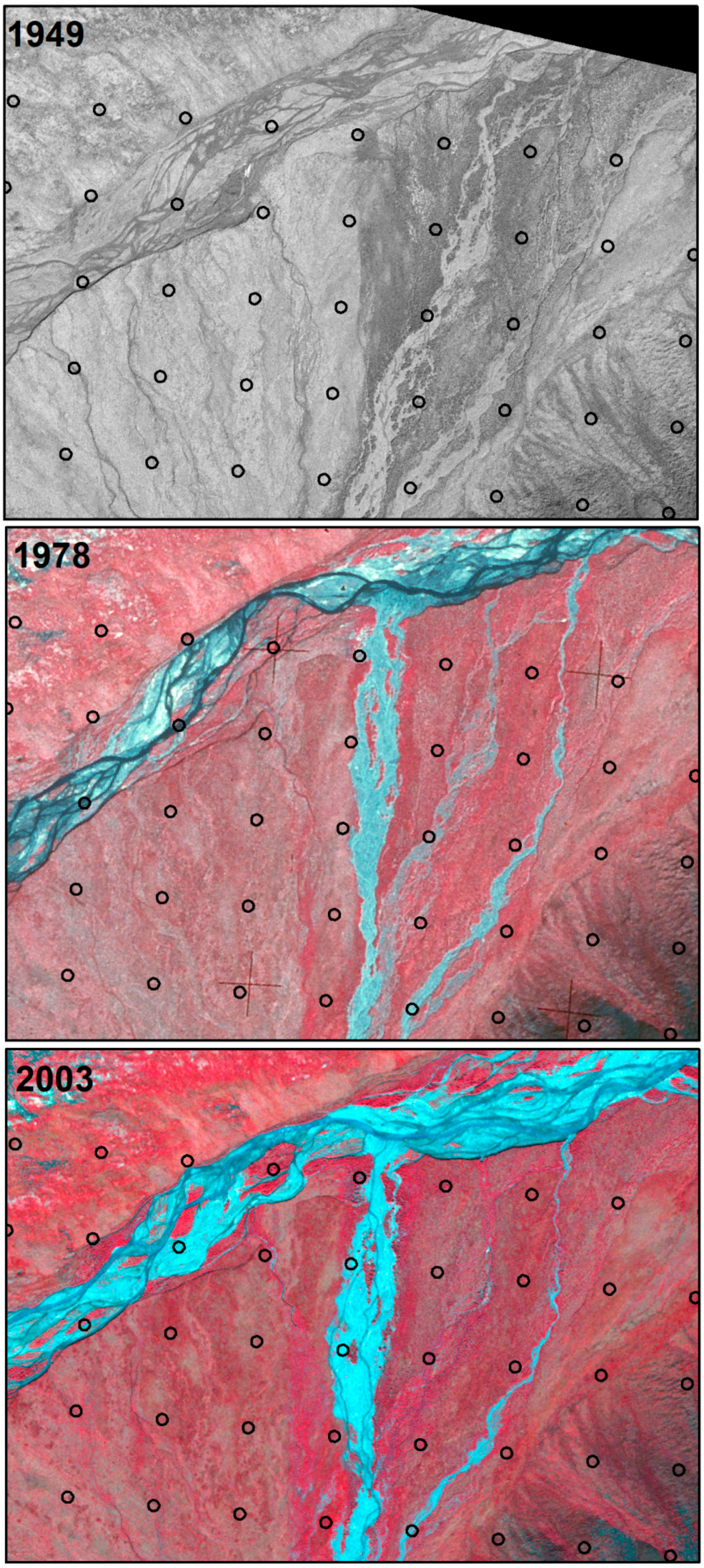

Figure A3. Time series of an alluvial fan in the northern Brooks Range, showing rerouting of creek on the fan and shrub changes along the creek as well as some shrub increase on the inactive parts of the fan. 2003 satellite image ©2018 DigitalGlobe, a Maxar company.

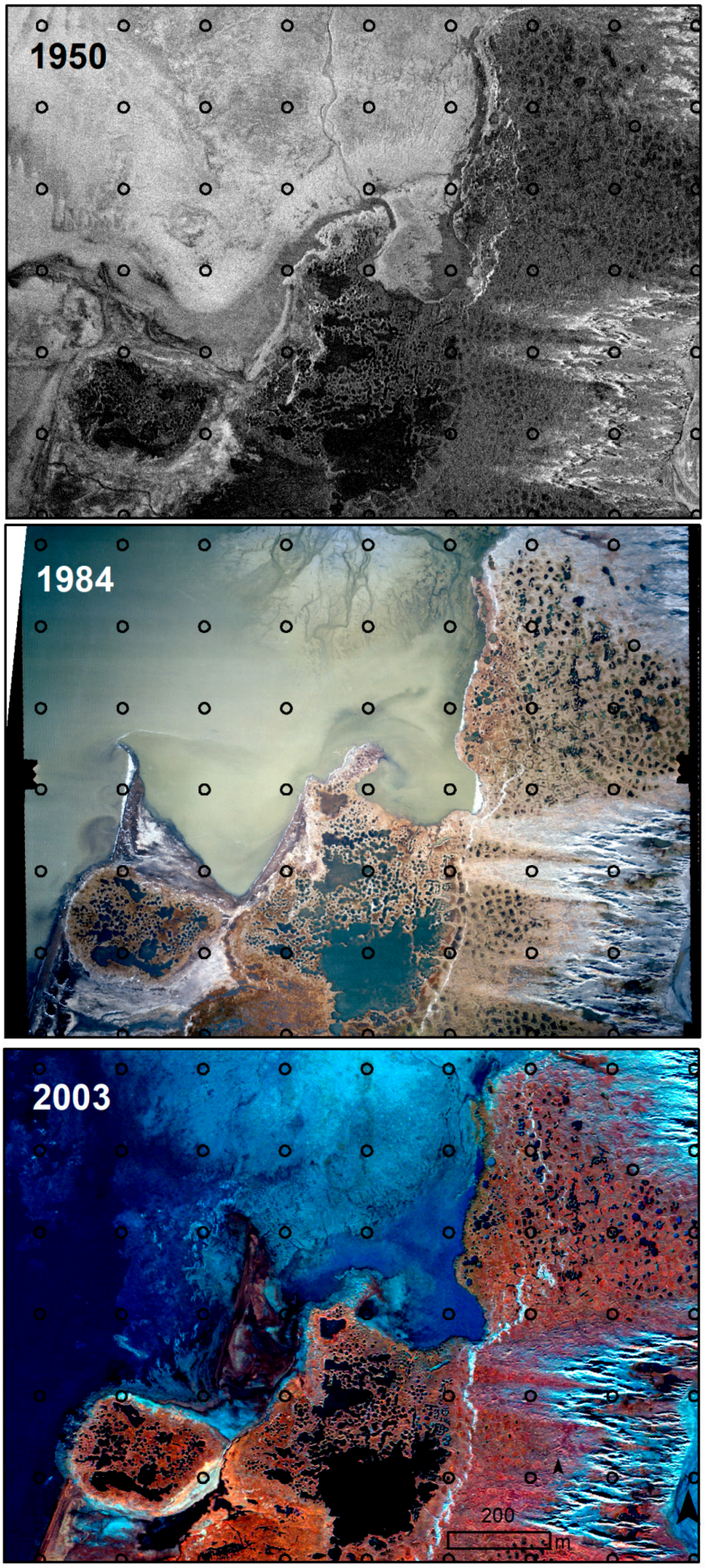

Figure A4. Time series of images at a coastal site showing salt marshes, long-shore sediment transport, moving drift wood lines from storm surges (right of center), and dunes (at right). 2003 satellite image ©2018 DigitalGlobe, a Maxar company.

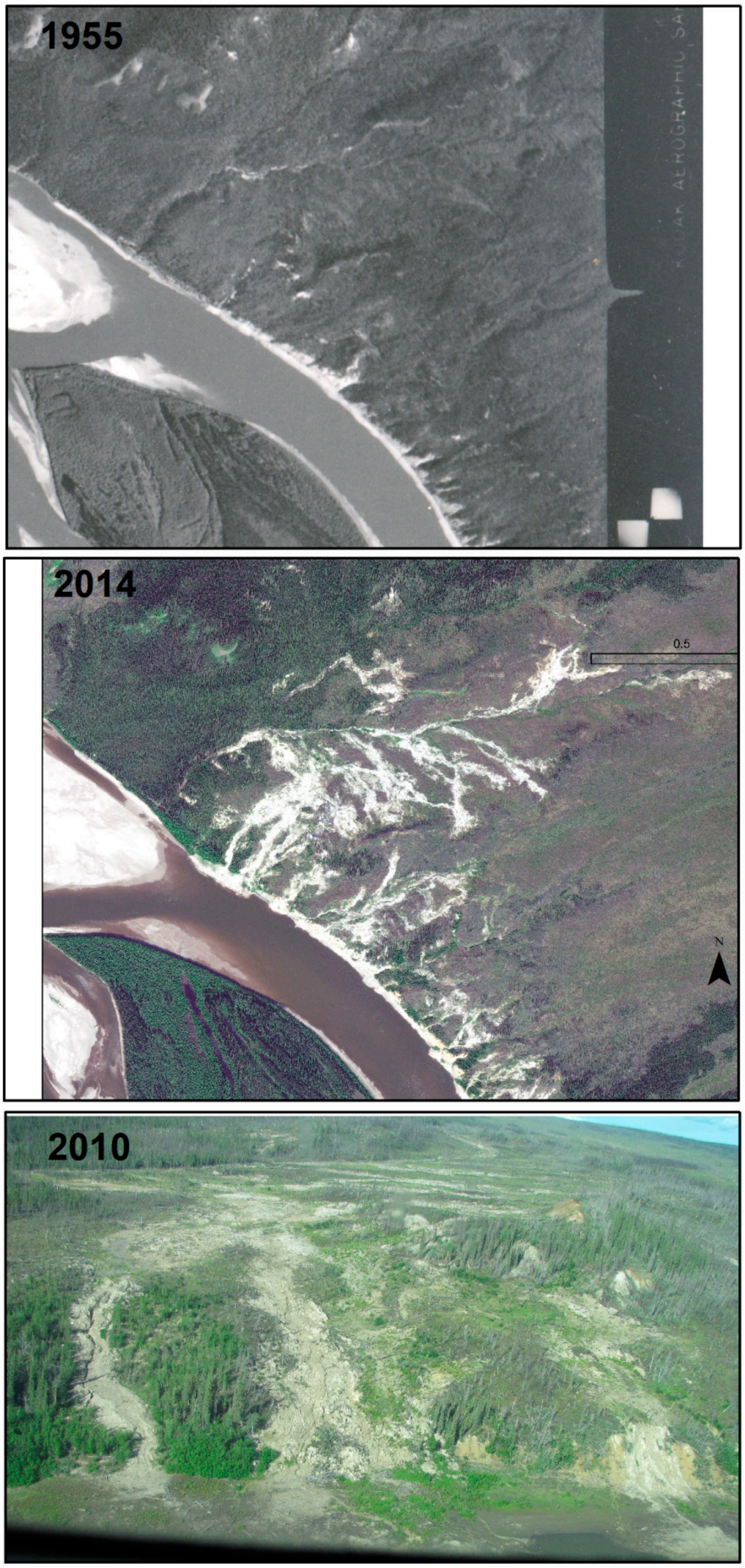

Figure A5. Active-layer detachment slides in spruce forest along the Porcupine River that burned in 2005. 2014 satellite image ©2018 DigitalGlobe, a Maxar company.

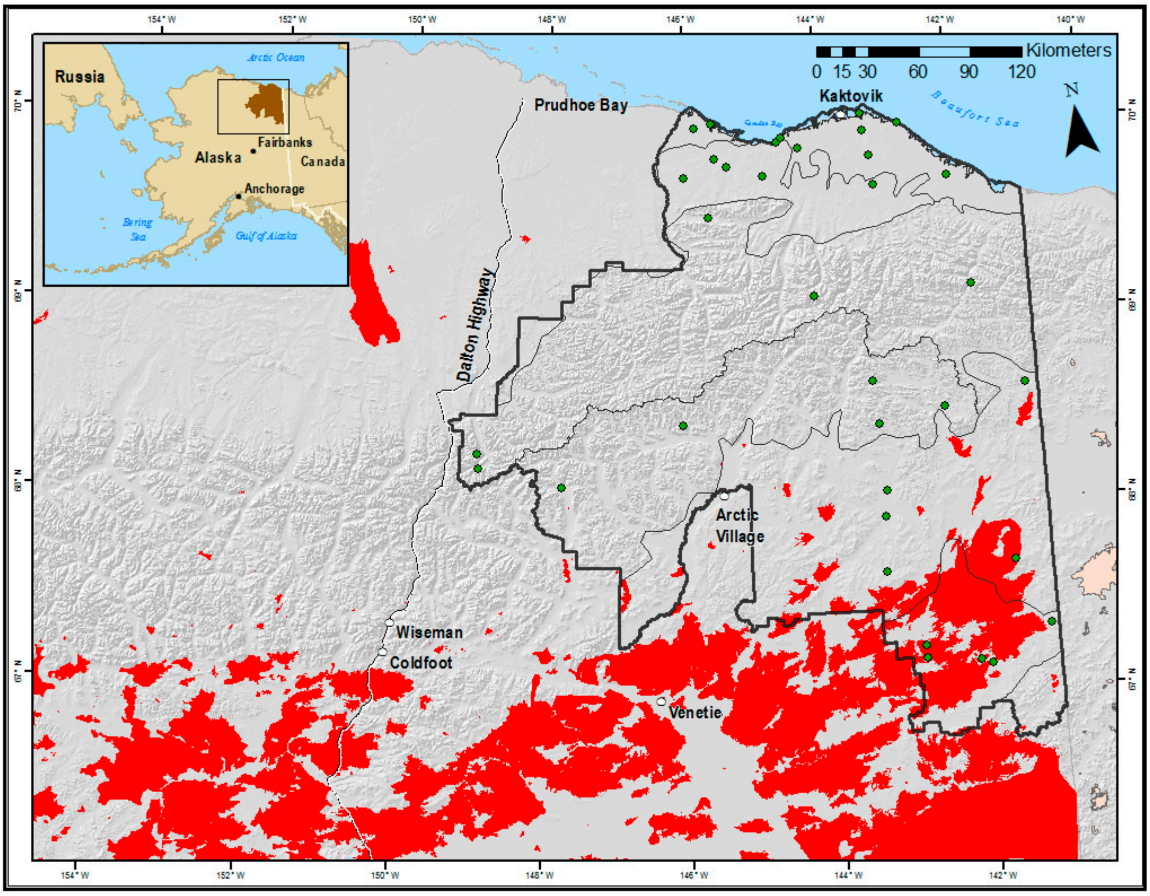

Figure A6. Map of recorded wildfires during 1950–2010 (in red) in the Arctic National Wildlife Refuge (black outline) and environs (Alaska Fire Service database). Green dots are study sites.

References

1. ACIA. *Impacts of a Warming Arctic: Arctic Climate Impact Assessment*; Cambridge University Press: Cambridge, UK, 2004; ISBN 0 521 61778 2.
2. Parson, E.A.; Carter, L.; Anderson, P.; Wang, B.; Weller, G.; Maccracken, M. Potential consequences of climate variability and change for Alaska. In *Climate Change Impacts on the United States*; Parson, E.A., Carter, L., Anderson, P., Wang, B., Weller, G., Maccracken, M., Eds.; U.S. Global Change Research Program: Washington, DC, USA, 2001; pp. 283–312. ISBN 0521000750.
3. Mantua, N.J.; Hare, S.R. The Pacific Decadal Oscillation. *J. Oceanogr.* **2002**, *58*, 35–44. [CrossRef]
4. Hartmann, B.; Wendler, G. The significance of the 1976 Pacific climate shift in the climatology of Alaska. *J. Clim.* **2005**, *18*, 4824–4839. [CrossRef]
5. Hinzman, L.; Bettez, N.; Bolton, B.; Chapin, F.S.; Dyurgerov, M.B.; Fastie, C.L.; Griffith, B.; Hollister, R.D.; Hope, A.; Huntington, H.P.; et al. Evidence and implications of recent climate change in terrestrial regions of the Arctic. *Clim. Chang.* **2005**, *72*, 251–298. [CrossRef]
6. Hinzman, L.D.; Deal, C.J.; McGuire, A.D.; Mernild, S.H.; Polyakov, I.V.; Walsh, J.E. Trajectory of the Arctic as an integrated system. *Ecol. Appl.* **2013**, *23*, 1837–1868. [CrossRef] [PubMed]
7. Gogineni, P.; Romanovsky, V.; Cherry, J.; Duguay, C.; Goetz, S.; Jorgenson, M.T.; Moghaddami, M. *Opportunities to Use Remote Sensing in Understanding Permafrost and Related Ecological Characteristics: Report of a Workshop*; National Academy of Science: Washington, DC, USA, 2014; p. 84. ISBN 978-0-309-30121-3.
8. Jorgenson, M.T.; Grosse, G. Remote sensing of landscape change in permafrost regions. *Permafr. Periglac. Processes* **2016**, *27*, 324–338. [CrossRef]

9. Bhatt, U.S.; Walker, D.A.; Raynolds, M.K.; Comiso, J.C.; Epstein, H.E.; Jia, G.; Gens, R.; Tweedie, C.E.; Tucker, C.J.; Webber, P.J. Circumpolar arctic tundra vegetation change is linked to sea ice decline. *Earth Interact.* **2010**, *14*, 1–20. [CrossRef]
10. Beck, P.S.A.; Goetz, S.J. Satellite observations of high northern latitude vegetation productivity changes between 1982 and 2008: Ecological variability and regional differences. *Environ. Res. Lett.* **2011**, *6*, 045501. [CrossRef]
11. Epstein, H.E.; Raynolds, M.K.; Walker, D.A.; Bhatt, U.S.; Tucker, C.J.; Pinzon, J.E. Dynamics of aboveground phytomass of the circumpolar arctic tundra over the past three decades. *Environ. Res. Lett.* **2012**, *7*, 015506. [CrossRef]
12. Jia, G.J.; Epstein, H.E.; Walker, D.A. Greening of arctic Alaska, 1981–2001. *Geophys. Res. Lett.* **2003**, *30*, 2067. [CrossRef]
13. Stow, D.A.; Hope, A.; Mcguire, D.; Verbyla, D.; Gamon, J.; Huemmrich, F.; Houston, S.; Racine, C.; Sturm, M.; Tape, K.; et al. Remote sensing of vegetation and land-cover change in arctic tundra ecosystems. *Remote Sens. Environ.* **2004**, *89*, 281–308. [CrossRef]
14. Frost, G.V.; Epstein, H.E. Tall shrub and tree expansion in Siberian tundra ecotones since the 1960s. *Glob. Chang. Biol.* **2014**, *20*, 1264–1277. [CrossRef] [PubMed]
15. Myers-Smith, I.H.; Forbes, B.C.; Wilmking, M.; Hallinger, M.; Lantz, T.C.; Block, D.; Tape, K.D.; Macias-Fauria, M.; Sass-Klaassen, U.; Lévesque, E. Shrub expansion in tundra ecosystems: Dynamics, impacts and research priorities. *Environ. Res. Lett.* **2011**, *6*, 045509. [CrossRef]
16. Bhatt, U.S.; Walker, D.A.; Raynolds, M.K.; Bieniek, P.A.; Epstein, H.E.; Comiso, J.C.; Pinzon, J.E.; Tucker, C.J.; Polyakov, I.V. Recent declines in warming and arctic vegetation greening trends over pan-arctic tundra. *Remote Sens.* **2013**, *5*, 4229–4254. [CrossRef]
17. Pattison, R.; Jorgenson, J.C.; Raynolds, M.K.; Welker, J. Trends in NDVI and tundra community composition in the arctic of NE Alaska between 1984 to 2009. *Ecosystems* **2015**, *18*, 707–719. [CrossRef]
18. Raynolds, M.K.; Walker, D.A.; Verbyla, D.; Munger, C.A. Patterns of change within a tundra landscape: 22-year landsat ndvi trends in an area of the northern foothills of the Brooks Range, Alaska. *Arct. Antarct. Alp. Res.* **2013**, *45*, 249–260. [CrossRef]
19. Elmendorf, S.C.; Henry, G.H.R.; Hollister, R.D.; Bjork, R.G.; Boulanger-Lapointe, N.; Cooper, E.J.; Cornelissen, J.H.C.; Day, T.A.; Dorrepaal, E.; Elumeeva, T.G.; et al. Plot-scale evidence of tundra vegetation change and links to recent summer warming. *Nat. Clim. Chang.* **2012**, *2*, 453–457. [CrossRef]
20. Jorgenson, J.C.; Raynolds, M.K.; Reynolds, J.H.; Benson, A.M. Twenty-five year record of changes in plant cover on tundra of northeastern Alaska. *Arct. Antarct. Alp. Res.* **2015**, *47*, 785–806. [CrossRef]
21. Jorgenson, M.T.; Shur, Y.L.; Pullman, E.R. Abrupt increase in permafrost degradation in arctic Alaska. *Geophys. Res. Lett.* **2006**, *33*, L02503. [CrossRef]
22. Johnstone, J.F.; Chapin, F.S., III; Hollingsworth, T.N.; Mack, M.C.; Romanovsky, V.; Turetsky, M. Fire, climate change, and forest resilience in interior Alaska. *Can. J. For. Res.* **2010**, *40*, 1302–1312. [CrossRef]
23. Kasischke, E.S.; Verbyla, D.L.; Rupp, T.S.; McGuire, A.D.; Murphy, K.A.; Jandt, R.; Barnes, J.L.; Hoy, E.E.; Duffy, P.A.; Calef, M.; et al. Alaska's changing fire regime—Implications for the vulnerability of its boreal forests. *Can. J. For. Res.* **2010**, *40*, 1313–1324. [CrossRef]
24. Riordan, B.; Verbyla, D.; McGuire, A.D. Shrinking ponds in subarctic Alaska based on 1950–2002 remotely sensed images. *J. Geophys. Res.* **2006**, *111*, G04002. [CrossRef]
25. Jones, B.M.; Grosse, G.; Arp, C.D.; Jones, M.C.; Walter Anthony, K.M.; Romanovsky, V.E. Modern thermokarst lake dynamics in the continuous permafrost zone, northern Seward Peninsula, Alaska. *J. Geophys. Res. Biogeosci.* **2011**, *116*, G00M03. [CrossRef]
26. Tape, K.; Sturm, M.; Racine, C. The evidence for shrub expansion in northern Alaska and the pan-arctic. *Glob. Chang. Biol.* **2006**, *12*, 686–702. [CrossRef]
27. Swanson, D.K. *Three Decades of Landscape Change in Alaska's Arctic National Parks: Analysis of Aerial Photographs C. 1980–2010*; National Park Service: Fort Collins, CO, USA, 2014; p. 29. Available online: https://www.sciencebase.gov/catalog/item/5771b8e2e4b07657d1a6d812 (accessed on 8 May 2018).
28. Naito, A.T.; Cairns, D.M. Patterns of shrub expansion in Alaskan arctic river corridors suggest phase transition. *Ecol. Evol.* **2015**, *5*, 87–101. [CrossRef] [PubMed]
29. Jorgenson, M.T.; Racine, C.H.; Walters, J.C.; Osterkamp, T.E. Permafrost degradation and ecological changes associated with a warming climate in central Alaska. *Clim. Chang.* **2001**, *48*, 551–579. [CrossRef]

30. Jorgenson, M.T.; Kanevksiy, M.Z.; Shur, Y.; Wickland, K.; Nossov, D.R.; Moskalenko, N.G.; Koch, J.; Striegl, R. Role of ground-ice dynamics and ecological feedbacks in recent ice-wedge degradation and stabilization. *J. Geophys. Res. Earth Surf.* **2015**, *120*, 2280–2297. [CrossRef]
31. Swanson, D.K. *Mapping of Erosion Features Related to Thaw of Permafrost in Bering Land Bridge National Preserve, Cape Krusenstern National Monument, and Kobuk National Park*; National Park Service: Fort Collins, CO, USA, 2010; p. 18. Available online: https://irma.nps.gov/DataStore/DownloadFile/446412 (accessed on 8 May 2018).
32. Shulski, M.; Wendler, G. *The Climate of Alaska*; University of Alaska Press: Fairbanks, AK, USA, 2007; ISBN 978-1602230071.
33. Jorgenson, J.C.; Joria, P.C.; Douglas, D.C. *Section 3: Land Cover*; Vol. Biological Science Report USGS/BRD/BSR-2002-0001; U.S. Geological Survey: Reston, VA, USA, 2002; pp. 4–7.
34. Nowacki, G.; Spencer, P.; Brock, T.; Fleming, M.; Jorgenson, T. *Ecoregions of Alaska and Neighboring Territories*; U.S. Geological Survey: Washington, DC, USA, 2001. Available online: https://agdc.usgs.gov/data/usgs/erosafo/ecoreg/index.html (accessed on 8 May 2018).
35. Viereck, L.A.; Dyrness, C.T.; Batten, A.R.; Wenzlick, K.J. *The Alaska Vegetation Classification. Pacific Northwest Research Station*; Vol. Gen. Tech. Rep. PNW-GTR-286; U.S. Forest Service: Portland, OR, USA, 1992; p. 278. Available online: https://www.fs.fed.us/pnw/publications/pnw_gtr286/pnw_gtr286a.pdf (accessed on 8 May 2018).
36. Jorgenson, M.T.; Grunblatt, J. *Landscape-Level Ecological Mapping of Northern Alaska and Field Site Photography*; Final Report prepared for Arctic Land Conservation Cooperative by Alaska Ecoscience, Fairbanks, AK, USA, and Geographic Information Network of Alaska; University of Alaska Fairbanks: Fairbanks, AK, USA, 2013; p. 48. Available online: https://lccnetwork.org/resource/landscape-level-ecological-mapping-northern-alaska-and-field-site-photography-report (accessed on 8 May 2018).
37. Pastick, N.J.; Wylie, B.K.; Jorgenson, M.T.; Goetz, S.J.; Jones, B.M.; Swanson, D.K.; Minsley, B.J.; Genet, H.; Knight, J.F.; Jorgenson, J.C. Spatiotemporal remote sensing of ecosystem change and causation across Alaska. *Glob. Chang. Biol.* **2018**, 1–19. [CrossRef] [PubMed]
38. Kasischke, E.S.; Turetsky, M.R. Recent changes in the fire regime across the North American boreal region—Spatial and temporal patterns of burning across Canada and Alaska. *Geophys. Res. Lett.* **2006**, *33*, L09703. [CrossRef]
39. Jones, B.M.; Breen, A.L.; Gaglioti, B.V.; Mann, D.H.; Rocha, A.V.; Grosse, G.; Walker, D.A. Identification of unrecognized tundra fire events on the north slope of Alaska. *J. Geophys. Res. Biogeosci.* **2013**, *118*, 1334–1344. [CrossRef]
40. Jones, B.M.; Kolden, C.A.; Jandt, R.; Abatzoglou, J.T.; Urban, F.; Arp, C.D. Fire behavior, weather, and burn severity of the 2007 Anaktuvuk River tundra fire, North Slope, Alaska. *Arct. Antarct. Alp. Res.* **2009**, *41*, 309–316. [CrossRef]
41. Jones, B.M.; Grosse, G.; Arp, C.D.; Liu, L.; Miller, E.A.; Hayes, D.J.; Larsen, C. Recent arctic tundra fire initiates widespread thermokarst development. *Sci. Rep.* **2015**, *5*, 15865. [CrossRef] [PubMed]
42. Brown, D.; Jorgenson, M.T.; Kielland, K.; Verbyla, D.L.; Prakash, A.; Koch, J.C. Landscape effects of wildfire on permafrost distribution in interior Alaska derived from remote sensing. *Remote Sens.* **2016**, *8*, 654. [CrossRef]
43. Nolan, M.; Arendt, A.; Rabus, B.; Hinzman, L. Volume change of McCall glacier, arctic Alaska, USA, 1956–2003. *Ann. Glaciol.* **2005**, *42*, 409–416. [CrossRef]
44. Epstein, H.E.; Myers-Smith, I.; Walker, D.A. Recent dynamics of arctic and sub-arctic vegetation. *Environ. Res. Lett.* **2013**, *8*, 015040. [CrossRef]
45. Swanson, D.K. Environmental limits of tall shrubs in Alaska's arctic national parks. *PLoS ONE* **2015**, *10*, e0138387. [CrossRef] [PubMed]
46. Tape, K.; Verbyla, D.; Welker, J. 20th century erosion in arctic Alaska foothills: The influence of shrubs, runoff, and permafrost. *J. Geophys. Res. Biogeosci.* **2011**, *116*, G04024. [CrossRef]
47. U.S. Boundary Commission. *Alaska-Canada Boundary Survey Map Set*; U.S. Geological Survey: Washington, DC, USA, 2011.
48. Harsch, M.A.; Hulme, P.E.; McGlone, M.S.; Duncan, R.P. Are treelines advancing? A global meta-analysis of treeline response to climate warming. *Ecol. Lett.* **2009**, *12*, 1040–1049. [CrossRef] [PubMed]

49. Liljedahl, A.K.; Boike, J.; Daanen, R.P.; Fedorov, A.N.; Frost, G.V.; Grosse, G.; Larry, D.H.; Yoshihiro, I.; Janet, C.J.; Nadya, M.; et al. Pan-arctic ice-wedge degradation in warming permafrost and its influence on tundra hydrology. *Nat. Geosci.* **2016**, *9*, 312–318. [CrossRef]
50. Swanson, D.K. Permafrost landforms as indicators of climate change in the arctic network of national parks. *Alaska Park Sci.* **2013**, *12*, 40–45.
51. Farquharson, L.M.; Mann, D.H.; Grosse, G.; Jones, B.M.; Romanovsky, V.E. Spatial distribution of thermokarst terrain in arctic Alaska. *Geomorphology* **2016**, *273*, 116–133. [CrossRef]
52. Jorgenson, M.T.; Shur, Y.L.; Osterkamp, T.E. Thermokarst in Alaska. In *Proceedings of the Ninth International Conference on Permafrost, Fairbanks, AK, USA, June 29–July 3 2008*; Kane, D.L., Hinkel, K.M., Eds.; Institute of Northern Engineering; University of Alaska: Fairbanks, AK, USA, 2008; pp. 869–876. ISBN 978-0-9800179-2-2.
53. Jorgenson, M.T.; Harden, J.; Kanevskiy, M.; O'Donnel, J.; Wickland, K.; Ewing, S.; Manies, K.; Zhuang, Q.; Shur, Y.; Striegl, R.; et al. Reorganization of vegetation, hydrology and soil carbon after permafrost degradation across heterogeneous boreal landscapes. *Environ. Res. Lett.* **2013**, *8*, 035017. [CrossRef]
54. Swanson, D.K. *Mapping of Erosion Features Related to Thaw of Permafrost in the Noatak National Preserve, Alaska*; National Park Service: Fort Collins, CO, USA, 2012; p. 28. Available online: https://irma.nps.gov/DataStore/DownloadFile/446412 (accessed on 8 May 2018).
55. Jorgenson, M.T.; Brown, J. Classification of the Alaskan Beaufort Sea coast and estimation of sediment and carbon inputs from coastal erosion. *GeoMarine* **2005**, *482*, 32–45. [CrossRef]
56. Jorgenson, M.T.; Jorgenson, J.C.; Macander, M.; Payer, D.; Morkill, A.E. Monitoring of Coastal Dynamics at Beaufort Lagoon in the Arctic National Wildlife Refuge, Northeast Alaska; Reports on Polar and Marine Research, Arctic Coastal Dynamics Report of an International Workshop, Potsdam, Germany, 26–30 November 2001. Available online: http://rep4-vm.awi.de/26592/1/BerPolarforsch2002413.pdf#page=28 (accessed on 8 May 2018).
57. Jones, B.M.; Arp, C.D.; Jorgenson, M.T.; Hinkel, K.M.; Schmutz, J.A.; Flint, P.L. Increase in the rate and uniformity of coastline erosion in arctic Alaska. *Geophys. Res. Lett.* **2009**, *36*, L03503. [CrossRef]
58. Roach, J.; Griffith, B.; Verbyla, D. Landscape influences on climate-related lake shrinkage at high latitudes. *Glob. Chang. Biol.* **2013**, *19*, 2276–2284. [CrossRef] [PubMed]
59. Necsoiu, M.; Dinwiddie, C.L.; Walter, G.R.; Larsen, A.; Stothoff, S.A. Multi-temporal image analysis of historical aerial photographs and recent satellite imagery reveals evolution of water body surface area and polygonal terrain morphology in Kobuk Valley National Park, Alaska. *Environ. Res. Lett.* **2013**, *8*, 16. [CrossRef]
60. Plug, L.J.; Walls, C.; Scott, B.M. Thermokarst lake changes from 1978–2001 on the Tuktoyaktuk Peninsula, western Canadian Arctic. *Geophys. Res. Lett.* **2008**, *35*, L03502. [CrossRef]
61. Pavelsky, T.M.; Zarnetske, J.P. Rapid decline in river icings detected in arctic Alaska: Implications for a changing hydrologic cycle and river ecosystems. *Geophys. Res. Lett.* **2017**, *44*, 3228–3235. [CrossRef]
62. Jorgenson, M.T.; Marcot, B.G.; Swanson, D.K.; Jorgenson, J.C.; DeGange, A.R. Projected changes in diverse ecosystems from climate warming and biophysical drivers in northwest Alaska. *Clim. Chang.* **2015**, *130*, 131–144. [CrossRef]
63. Sormunen, H.; Virtanen, R.; Luoto, M. Inclusion of local environmental conditions alters high-latitude vegetation change predictions based on bioclimatic models. *Polar Biol.* **2011**, *34*, 883–897. [CrossRef]